What are the properties of a spin polarized unitary Fermi gas?

Aurel Bulgac
University of Washington

Collaborator*:*   Michael M. Forbes - UW

Why would one want to study a unitary gas?

One reason: for the nerds, I mean the hard-core theorists, not the phenomenologists.

What are the ground state properties of the many-body system composed of spin ½ fermions interacting via a zero-range, infinite scattering length contact interaction.

Bertsch's Many-Body X challenge, Seattle, 1999

This is a slightly idealized model for dilute neutron matter with an attractive two-body interaction. In neutron star crust $k_F|a| = O(10)$ and $|a|/r_0 \approx O(10)$ and this is a strongly interactive Fermi system and naïve models fail.

$$r_0 \ll n^{-1/3} \approx \frac{\pi}{k_F} \ll |a|$$

$$\sigma(k) = \frac{4\pi a^2}{1 + k^2 a^2} \approx \frac{4}{\pi n^{2/3}}$$

Lecture Notes in Physics 836

Wilhelm Zwerger *Editor*

The BCS-BEC Crossover and the Unitary Fermi Gas

Springer

At the crossroads of:

- **Atomic physics**
- **Atomic traps**
- **Laser physics**
- **Few body physics**
- **Condensed matter physics**
- **Low temperature physics**
- **Nuclear physics**
- **Neutron stars**
- **Relativistic heavy-ion physics**
- **Conformal field theory**
- **Effective field theory**

What are the scattering length and the effective range?

$$k \cotan \delta_0 = -\frac{1}{a} + \frac{1}{2} r_0 k^2 + \cdots$$

$$\sigma = \frac{4\pi}{k^2} \sin^2 \delta_0 + \cdots = 4\pi a^2 + \cdots$$

If the energy is small, only the s-wave scattering is relevant.

Let us consider a very old and simple example:

The hydrogen atom.

The ground state energy could only be a function of:

✓ **Electron charge**
✓ **Electron mass**
✓ **Planck's constant**

and then trivial dimensional arguments lead to

$$E_{gs} = \frac{e^4 m}{\hbar^2} \times \frac{1}{2}$$

Only the factor ½ requires some hard work.
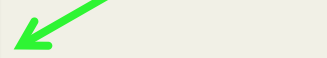
Let us turn now to dilute fermion matter

The ground state energy is given by a function:

$$E_{gs} = f(N, V, \hbar, m, a, r_0)$$

Taking the scattering length to infinity and the range of the interaction to zero, we are left with:

Pure number

$$E_{gs} = F(N, V, \hbar, m) = \frac{3}{5} \varepsilon_F N \times \boxed{\xi}$$

if $\xi > 0$ - the system is a gas with positive presure

if $\xi < 0$ - the system collapses, since presure is negative

$$\varepsilon_F = \frac{\hbar^2 k_F^2}{2m}, \quad n = \frac{N}{V} = \frac{k_F^3}{3\pi^2}$$

George actually wanted to know the sign of ξ.

In 1999 we did not know the sign of ξ!

There were a number of papers making opposite claims around that time.

➢ **G.A. Baker, Jr (LANL) won the $600 prize**
($300 from George + $300 from V.A. Khodel)
   **Phys. Rev. C 60, 064901 (1999)**

The Bertsch, nonparametric model of neutron matter is analyzed and strong indications are found that, in the infinite system limit, the ground state is a Fermi liquid with an effective mass, except for a set of measure zero.

➢ **H. Heiselberg, second runner-up**
   Phys. Rev. A 63, 043606 (2001)

Ground-state energies and superfluid gaps are calculated for degenerate Fermi systems interacting via long attractive scattering lengths such as cold atomic gases, neutron, and nuclear matter. In the Intermediate region of densities, where the interparticle spacing ($\sim 1/k_F$) is longer than the range of the interaction but shorter than the scattering length, the superfluid gaps and the energy per particle are found to be proportional to the Fermi energy and thus differ from the dilute and high-density limits. The attractive potential increase linearly with the spin-isospin or hyperspin statistical factor such that, e.g., symmetric nuclear matter undergoes spinodal decomposition and collapses whereas neutron matter and Fermionic atomic gases with two hyperspin states are mechanically *stable* in the intermediate density region. The regions of spinodal instabilities in the resulting phase diagram are reduced and do not prevent a superfluid transition.

Observation of a Strongly Interacting Degenerate Fermi Gas of Atoms
O'Hara, Hemmer, Gehm, Granade, and Thomas
Science, 298, 2179 (2002)
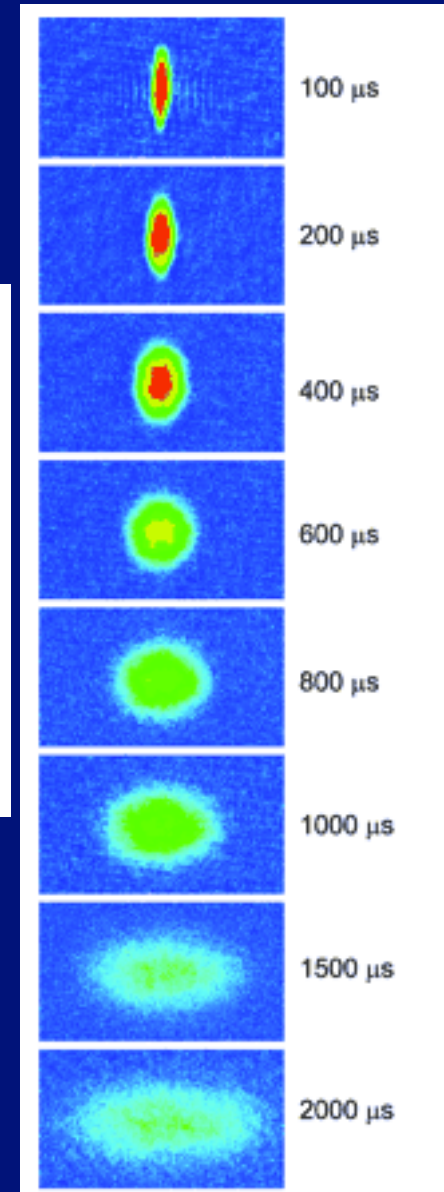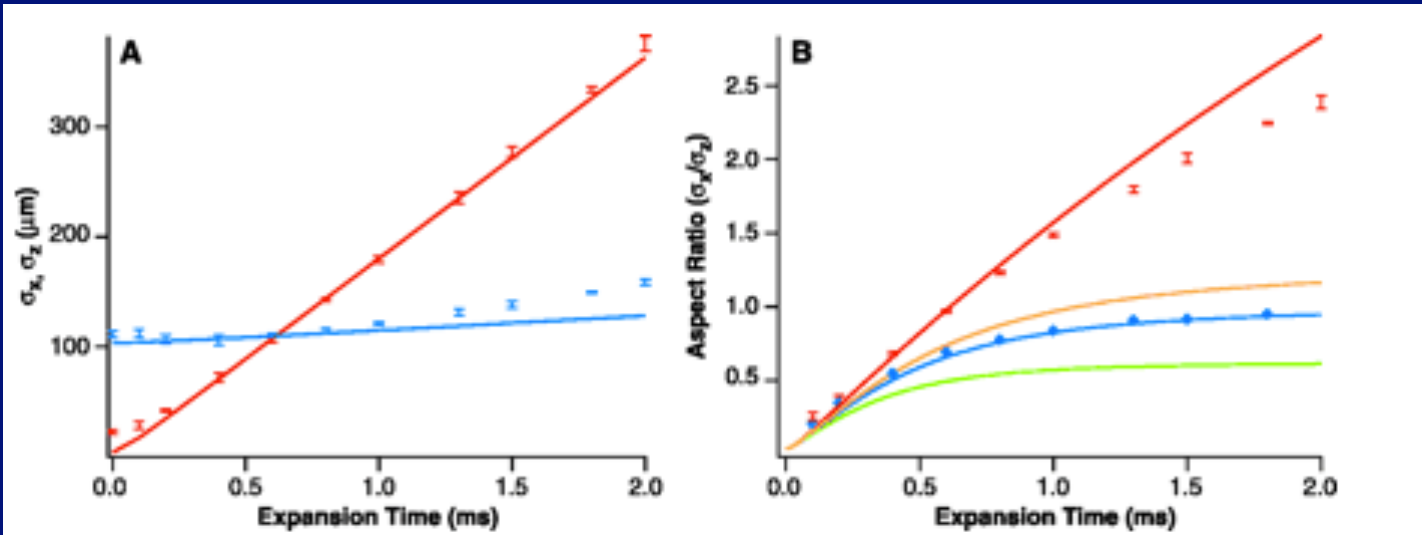
The atomic cloud expansion is similar to that observed in RHIC heavy-ion collisions.

Superfluid Fermi Gases with Large Scattering Length
Carlson, Chang, Pandharipande, and Schmidt
Phys. Rev. Lett. <u>91</u>, 050401 (2003)

We report quantum Monte Carlo calculations of superfluid Fermi gases with short-range two-body attractive interactions with infinite scattering length. The energy of such gases is estimated to be 0:44 ±0:01 times that of the non-interacting gas, and their pairing gap is approximately twice the energy per particle.
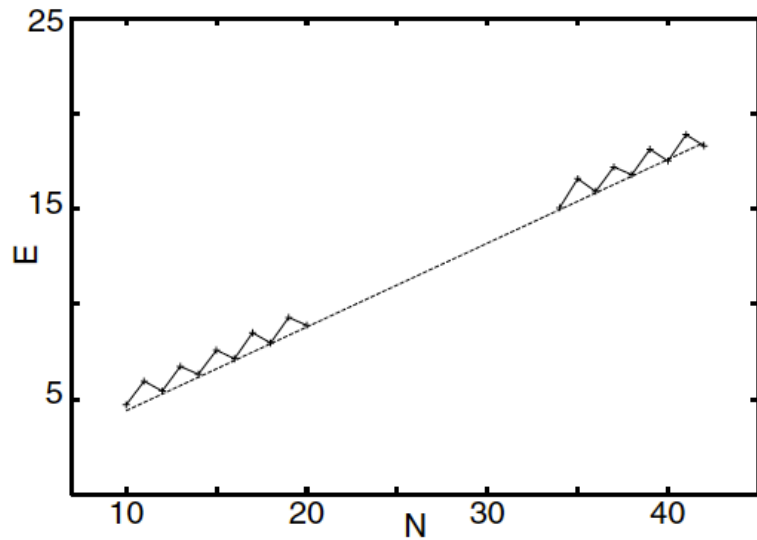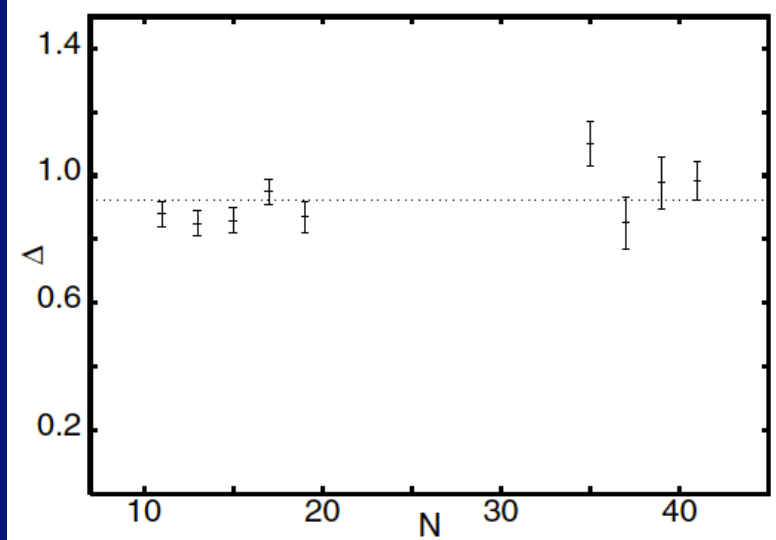
FIG. 3. The $E(N)$ in units of E_{FG}.

FIG. 4. The gap in units of E_{FG}.

$$E_{FG} = \frac{E}{N} = \frac{3\hbar^2 k_F^2}{10m}, \qquad n = \frac{N}{V} = \frac{k_F^3}{3\pi^2}$$

Why should one study fermionic superfluidity?

Superconductivity (which turned 100 years old on April 8th, 2011) and superfluidity in Fermi systems are manifestations of quantum coherence at a macroscopic level

- ✓ **Dilute atomic Fermi gases** $T_c \approx 10^{-9}$ eV

- ✓ **Liquid ^{3}He** $T_c \approx 10^{-7}$ eV

- ✓ **Metals, composite materials** $T_c \approx 10^{-3} - 10^{-2}$ eV

- ✓ **Nuclei, neutron stars** $T_c \approx 10^5 - 10^6$ eV

- • **QCD color superconductivity** $T_c \approx 10^7 - 10^8$ eV

units (1 eV ≈ 10^4 K)

Vortices and Superfludity in a strongly interacting Fermi gas
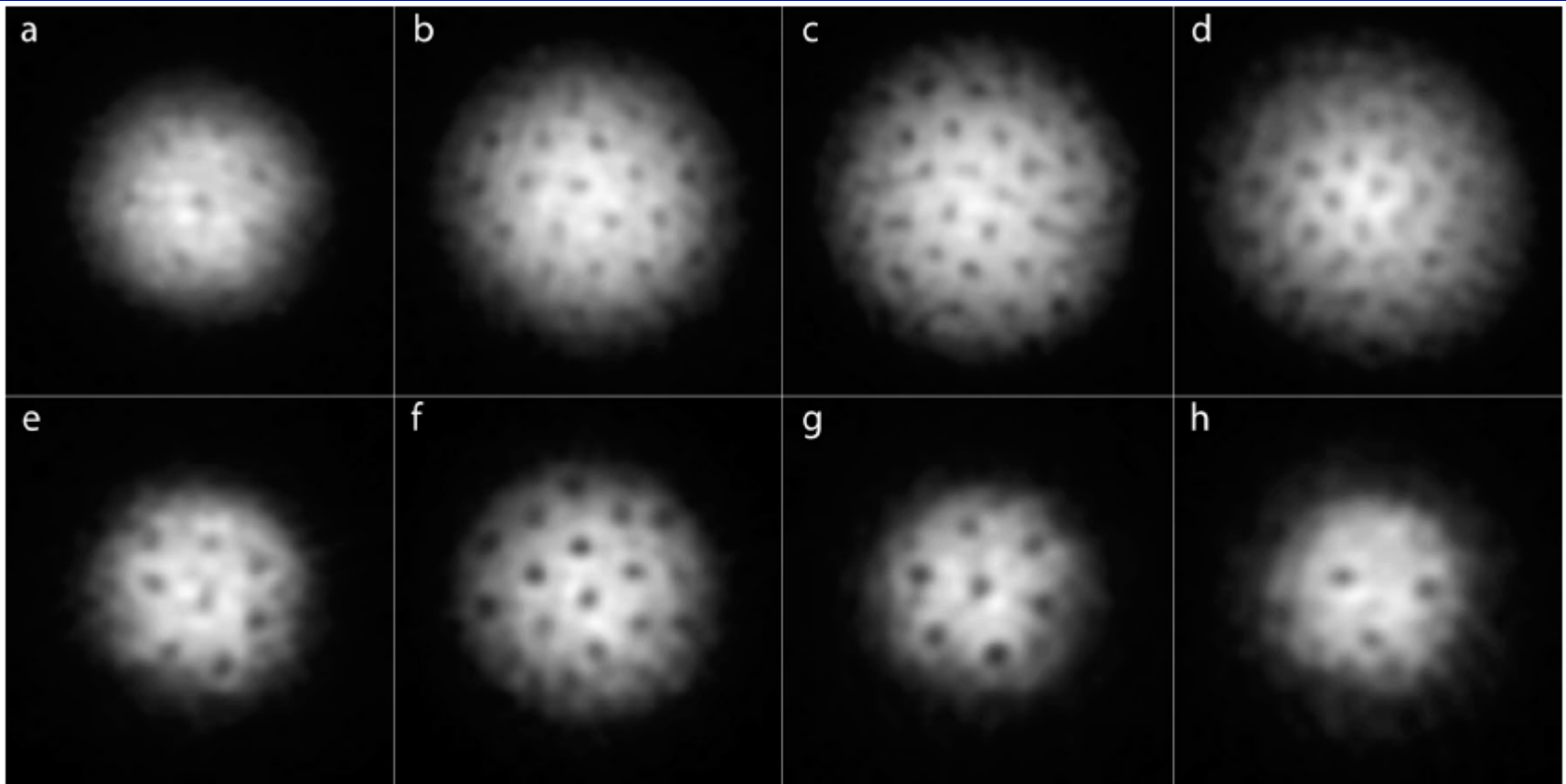## Zwierlein, Abo-Shaeer, Schirotzek, Schunck, and Ketterle, Nature 435, 1047(2005)

Fig. 2: Vortices in a strongly interacting gas of fermionic atoms on the BEC- and the BCS-side of the Feshbach resonance. At the given field, the cloud of lithium atoms was stirred for 300 ms (a) to 500 ms (b-h) followed by an equilibration time of 500 ms. After 2 ms of ballistic expansion, the magnetic field was ramped to 735 G for imaging (see text for details). The magnetic fields were (a) 740 G, (b) 766 G, (c) 792 G, (d) 812 G, (e) 833 G, (f) 843 G, (g) 853 G and (h) 863 G. The field of view of each image is $880 \ \mu m \times 880 \ \mu m$.

Superfluid pairing in neutrons and cold atoms
Carlson, Gandolfi, and Gezerlis, arXiv:1204.2596
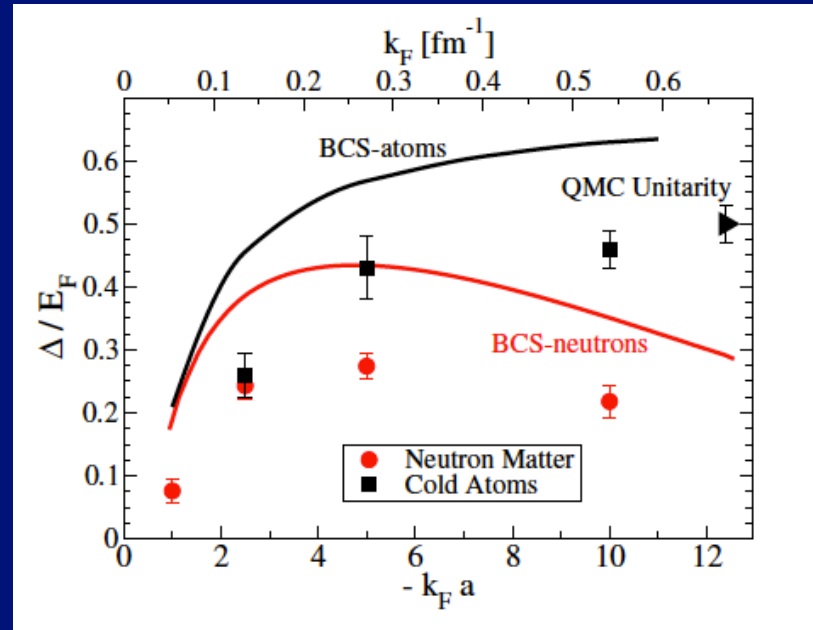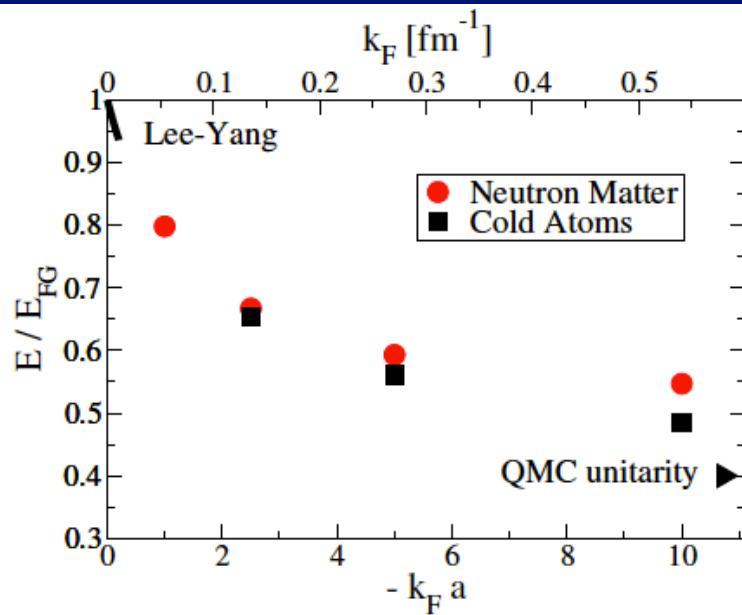
$$E_{FG} = \frac{E}{N} = \frac{3\hbar^2 k_F^2}{10m}, \qquad n = \frac{N}{V} = \frac{k_F^3}{3\pi^2}$$
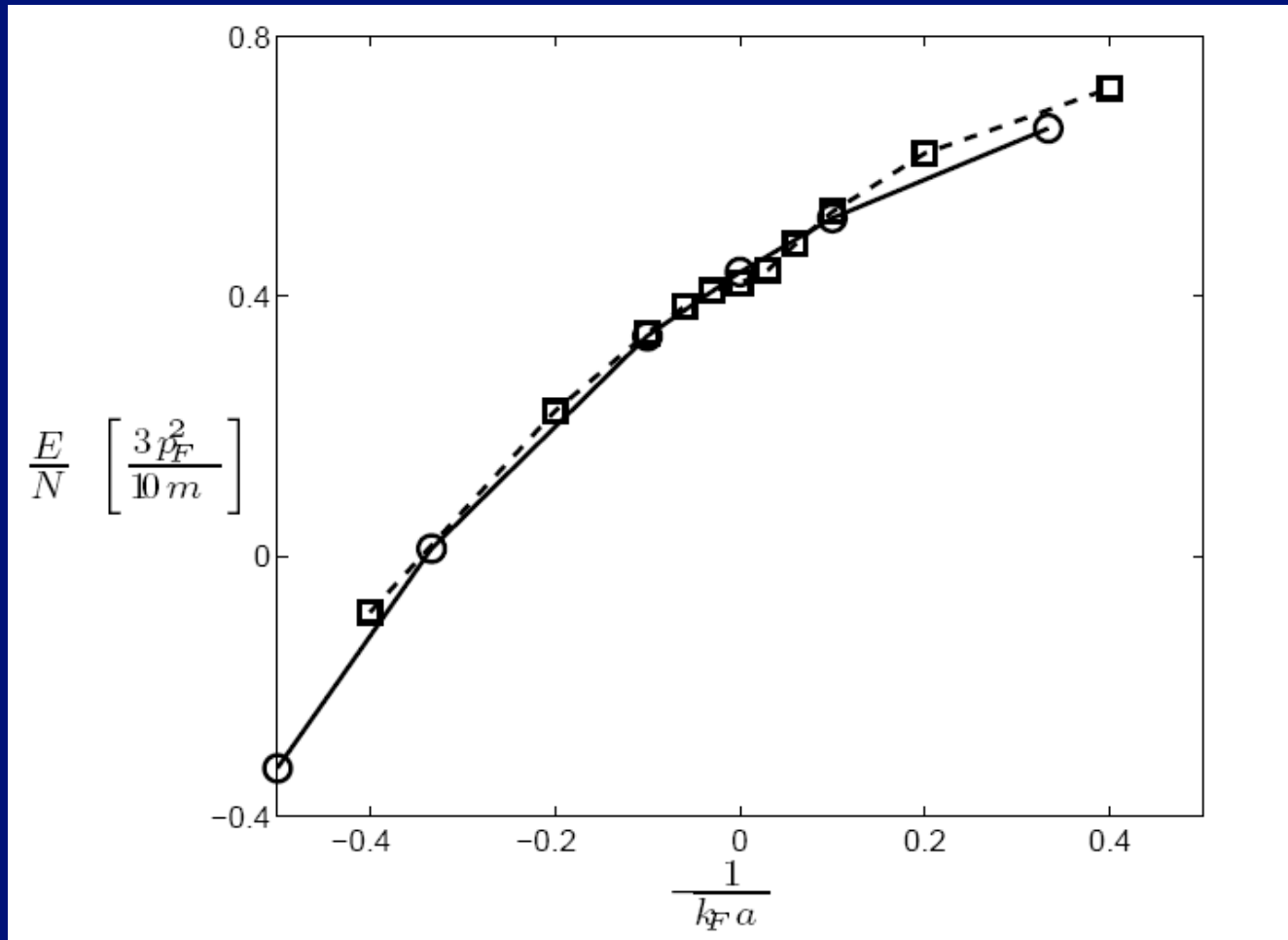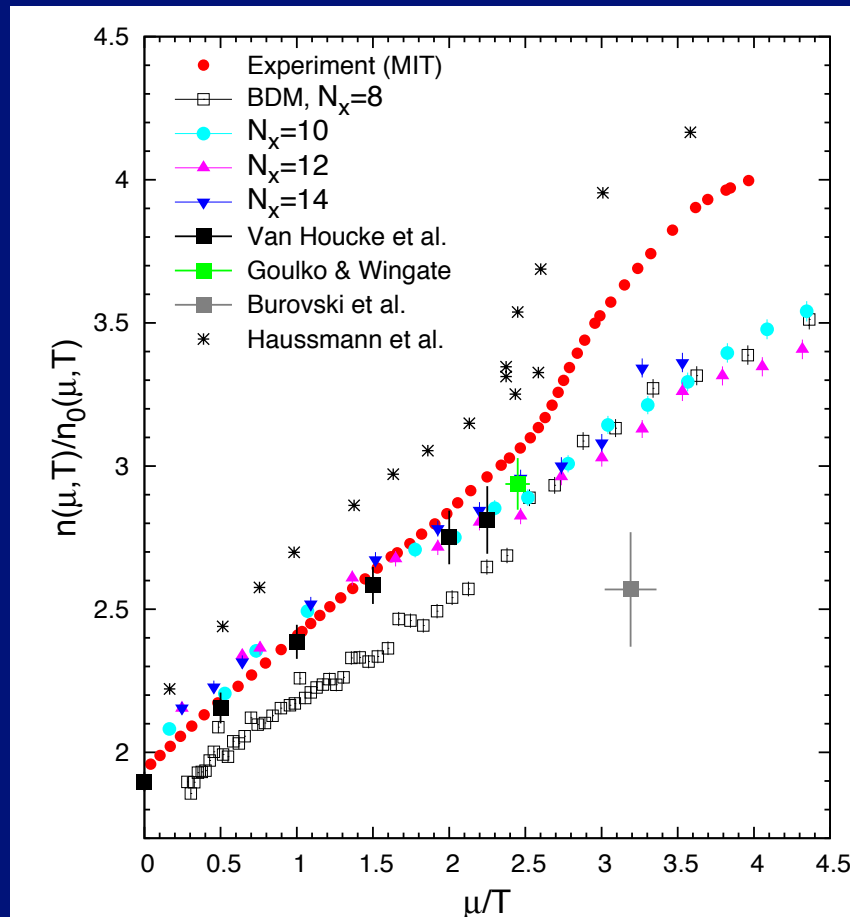
BEC side **BCS side**

Solid line with open circles – Chang *et al.* PRA, 70, 043602 (2004)
Dashed line with squares - Astrakharchik *et al.* PRL 93, 200404 (2004)

Theory versus experiment for Equation of State

Ku, Sommer, Cheuk, and Zwierlein, Science, 335, 563 (2012)
Bulgac, Drut, and Magierski – (BDM, N_x= 8), Phys. Rev. Lett. 96, 090404 (2006)
Burovski, Prokofiev, Svistunov, and Troyer, Phys. Rev. Lett. 96, 160502 (2006)
Drut, Lahde, Wlazlowski, and Magierski – (N_x= 10, 12, 14), Phys. Rev. A 80, 051601(R) (2012)
Goulko and Wingate, Phys. Rev. A 82, 053621 (2010)
Van Houcke, … , Zwierlein, Nature Physics, 8, 366 (2012)
Haussmann and Zwerger, Phys. Rev. A 78, 063602 (2008)

Institutions working with atomic Fermi gases

Institute, country	Head of laboratory	Atom	Year of the first result, reference
JILA, USA	Deborah Jin	^{40}K	1999 [1]
Rice Univ., USA	Randall Hulet	^{6}Li	2001 [71]
Ecole Normale Supérieure, France	Christophe Salomon	^{6}Li	2001 [72]
Duke Univ., then North Carolina State Univ., USA	John Thomas	^{6}Li	2002 [66]
MIT, USA	Wolfgang Ketterle	^{6}Li	2002 [73]
Univ. Firenze, Italy	Massimo Inguscio	^{40}K	2002 [74]
Univ. Innsbruck, Austria	Rudolf Grimm	^{6}Li, ^{40}K	2003 [75]
Eidgenössische Technische Hochschule, Switzerland	Tilman Esslinger	^{40}K, ^{6}Li	2005 [76]
Tübingen Univ., Germany	Claus Zimmermann	^{6}Li	2005 [77]
Vrije Univ., The Netherlands	Wim Vassen	^{3}He	2006 [78]
Kyoto Univ., Japan	Yoshiro Takahashi	^{173}Yb, ^{171}Yb, ^{6}Li	2007 [79]
Swinburne Univ. Technology, Australia	Christopher Vale	^{6}Li	2007 [80]
Univ. Electro-Communications, Japan	Takashi Mukaiyama	^{6}Li	2008 [81]
Max Planck Inst. Kernphysik, then Univ. Heidelberg, Germany	Selim Jochim	^{6}Li	2008 [15]
Pennsylvania State Univ., USA	Kenneth O'Hara	^{6}Li	2009 [82]
MIT, USA	Martin Zwierlein	^{6}Li, ^{40}K	2009 [83]
Institute of Applied Physics, Russian Academy of Sciences, Russia	Andrey Turlapov	^{6}Li	2010 [16]
Rice Univ., USA	Thomas Killian	^{87}Sr	2010 [84]
Univ. Cambridge, United Kingdom	Michael Köhl	^{40}K	2011 [85]
Univ. Washington, USA	Subhadeep Gupta	^{6}Li	2011 [86]

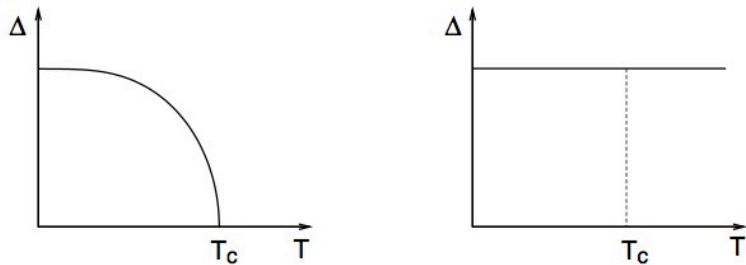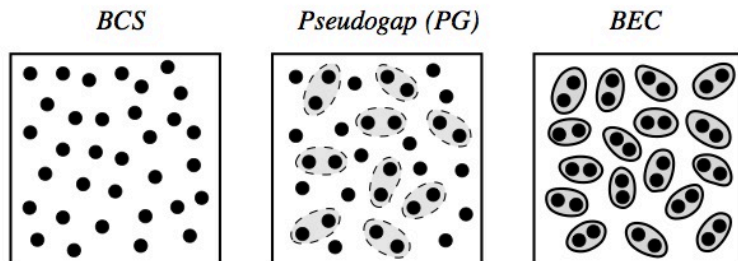# Unitary Fermi gases are unconventional fermionic superfluids
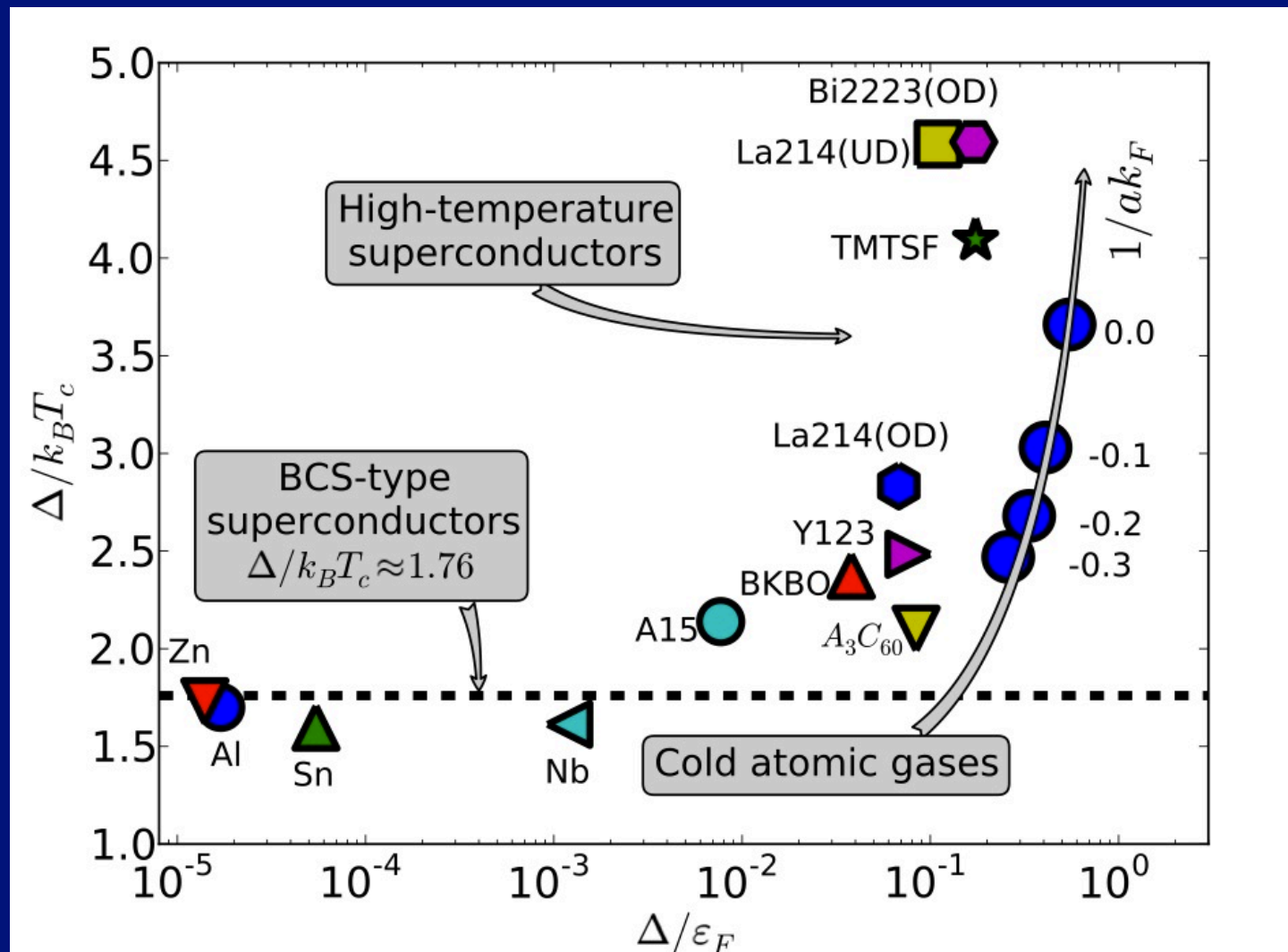
FIG. 4 Comparison of typical temperature dependences of the excitation gaps in the BCS (left) and BEC (right) limits. For the former, the gap is small and vanishes at T_c; whereas for the latter, the gap is very large and essentially temperature independent.
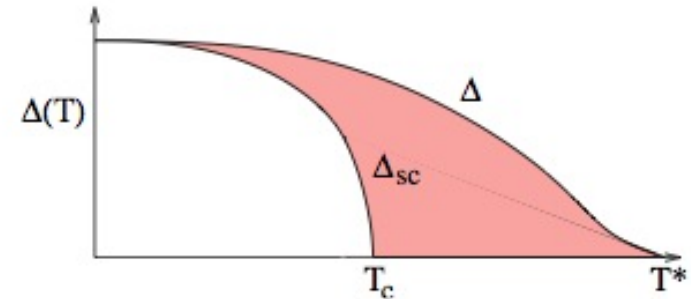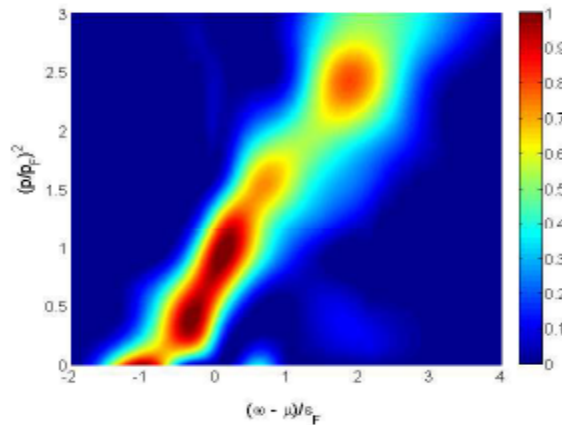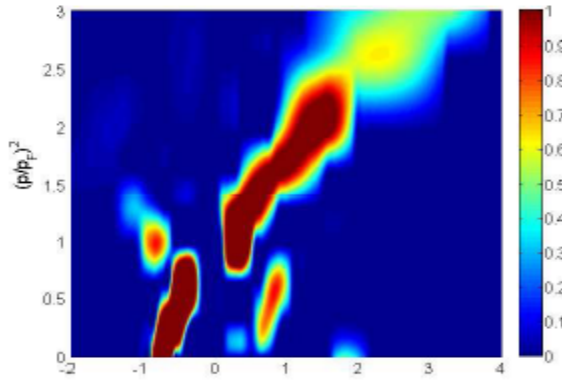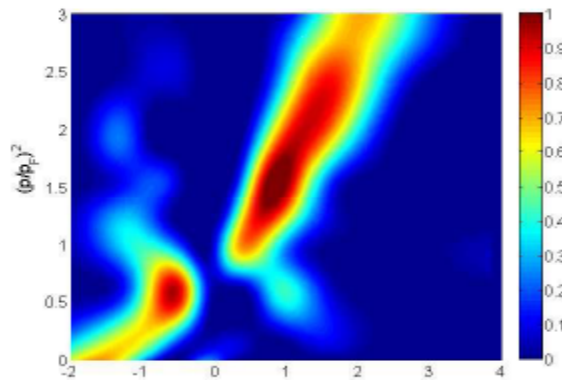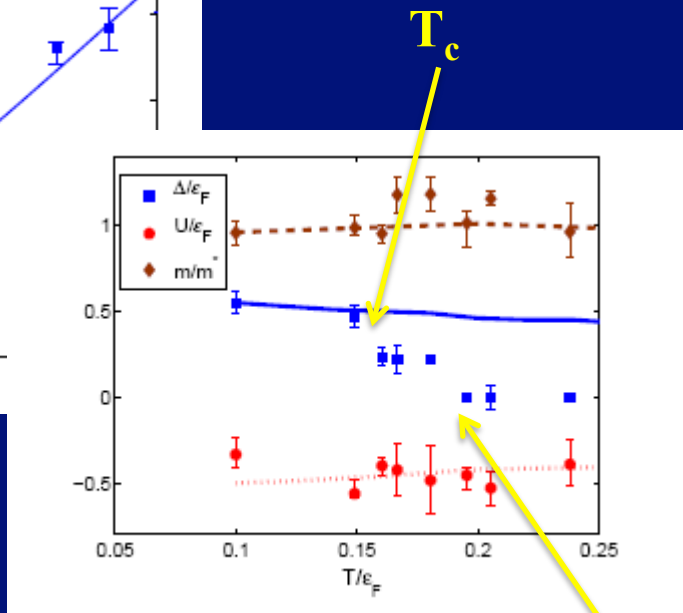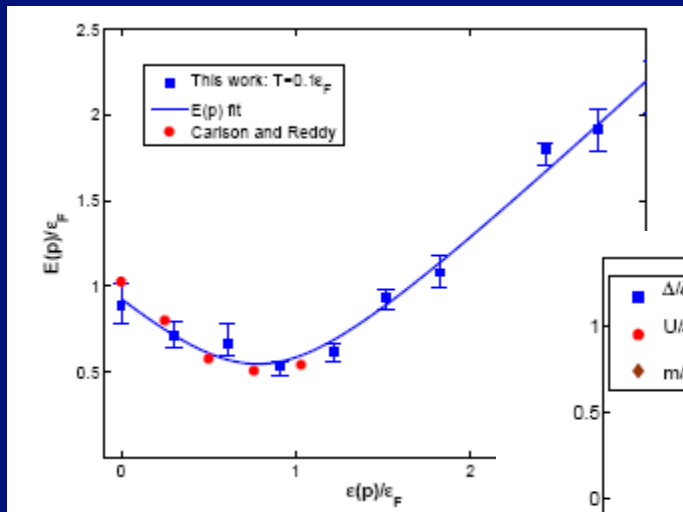
BCS   Pseudogap (PG)   BEC

T>T$_c$

FIG. 3 Contrasting behavior of the excitation gap $\Delta(T)$ and superfluid order parameter $\Delta_{sc}(T)$ versus temperature. The height of the shaded region roughly reflects the density of noncondensed pairs at each temperature.

$$G(p,\tau) = \frac{1}{Z}\text{Tr}\left\{\exp\left[-(\beta-\tau)(H-\mu N)\right]\psi^\dagger(p)\times\right.$$

$$\left.\exp\left[-\tau(H-\mu N)\right]\psi(p)\right\}$$

$$= -\frac{1}{2\pi}\int_{-\infty}^{\infty} d\omega A(p,\omega)\frac{\exp(-\omega\tau)}{1+\exp(-\omega\beta)}$$

T_c

The pseudo-gap vanishes at T_0

Magierski, Wlazlowski, Bulgac, and Drut
Phys. Rev. Lett. 103, 210403 (2009), arXiv:0801.1504
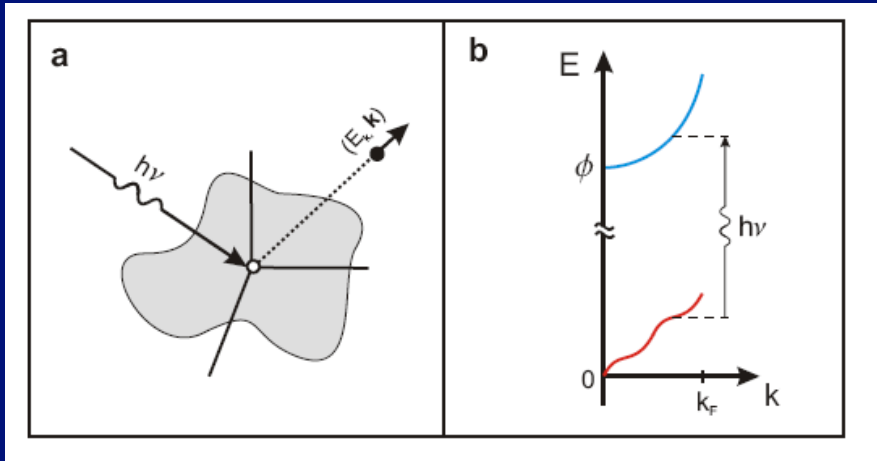
$$E(N) + h\nu = E(N-1) + E_k + \frac{\hbar^2 k^2}{2m} + \phi$$
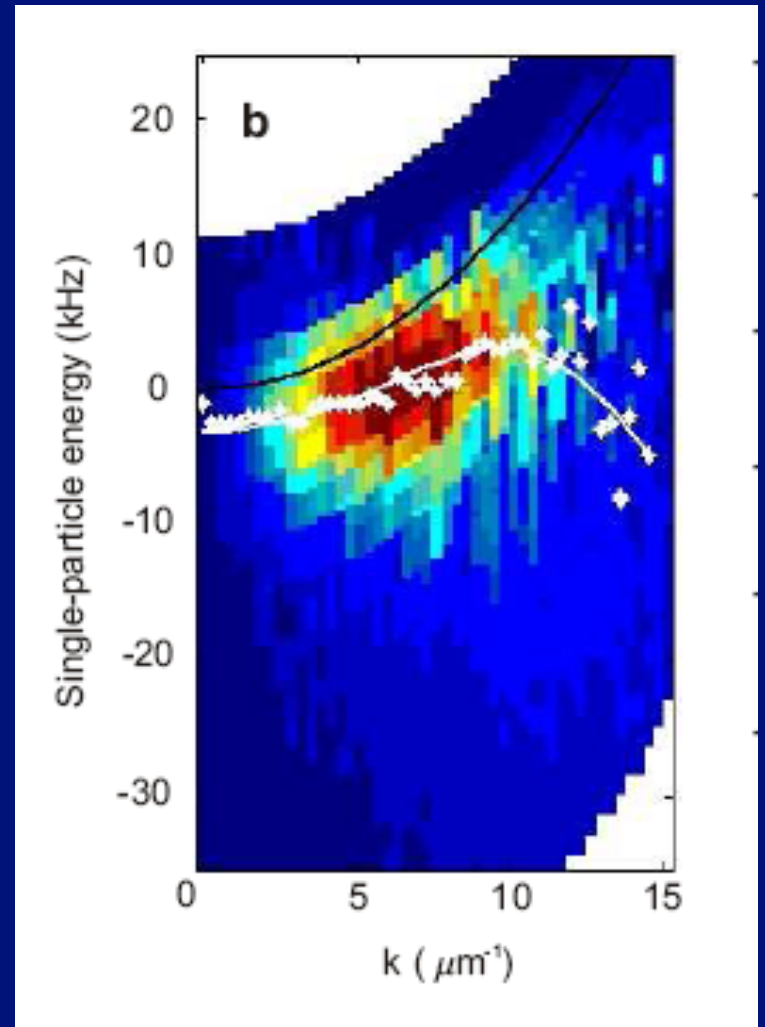
Using photoemission spectroscopy to probe a strongly interacting Fermi gas
Stewart, Gaebler, and Jin, Nature, <u>454</u>, 744 (2008)

FIG. 3 (color online). The gap Δ/ε_F extracted from the spectral weight function as a function of temperatur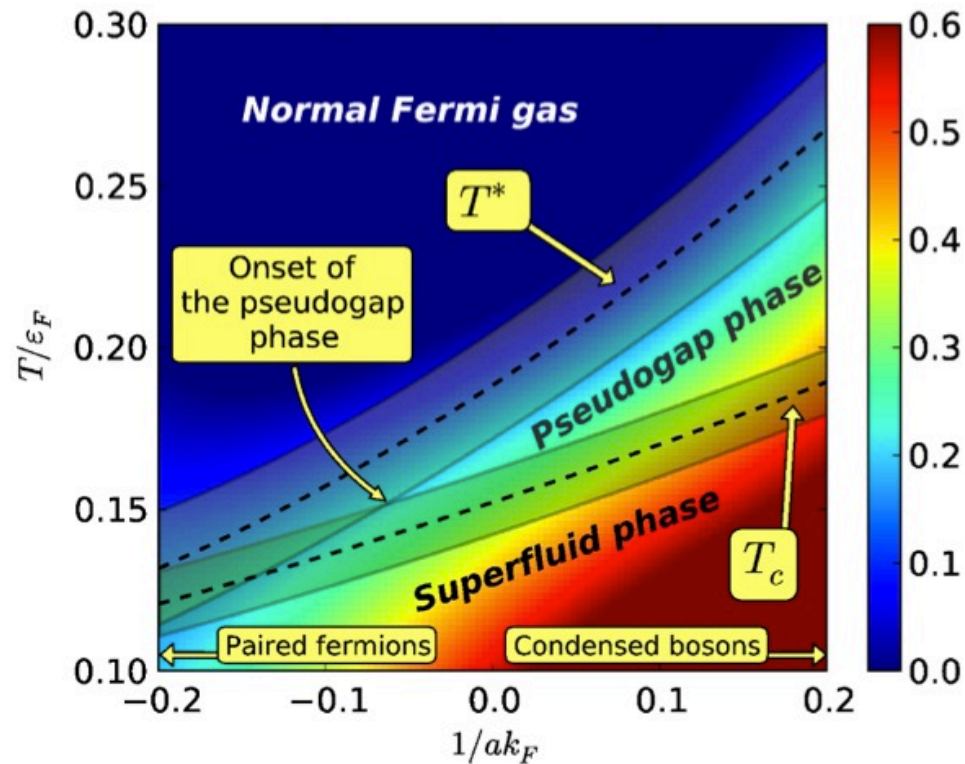e and scattering length. The dashed lines denote two temperatures: critical temperature T_c and the crossover temperature T^*. Uncertainties (both systematic and statistic errors, estimated to be no more than 10%) of these temperatures, are denoted by shaded area.

The onset of the pseudo-gap phase in ultracold Fermi gases
Magierski, Wlazlowski, and Bulgac, Phys. Rev. Lett. 107, 145304 (2011)

Shear viscosity of a unitary Fermi gas
(the only complete ab initio calculation in a Fermi system)

FIG. 3: (Color online) The ratio of the shear viscosity to the entropy density η/s as a function of dimensionless temperature for 8^3-lattice (red) squares and 10^3-lattice (blue) circles. The error bars only presents the stability of the combined (SVD and MEM) analytic continuation procedure with respect to the change of algorithm parameters, and do not include systematic errors of the entropy determination. By (red) dotted line conservative estimation for the upper bound is depicted. Result of the T-matrix theory are plotted by open (purple) circles [15]. In the high and low temperatures regime known asymptotics are depicted: for $T > 0.3\varepsilon_F$ by (green) line prediction of the kinetic theory and for $T < 0.2\varepsilon_F$ by (brown) line contribution from phonon excitations [13]. By dashed (black) line the KSS bound is plotted.
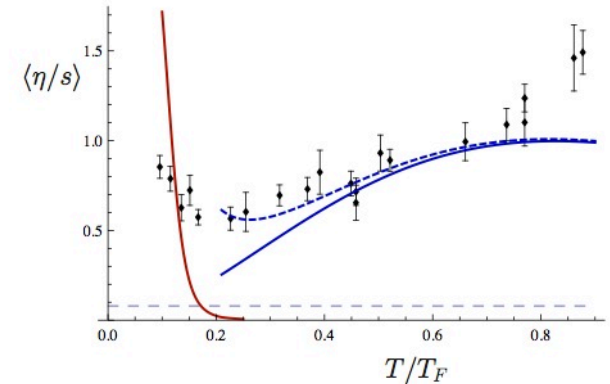
Lower limit for "perfect liquid"

Fig. 11 Trap average $\langle \alpha_s \rangle = \langle \eta/s \rangle$ extracted from the damping of the radial breathing mode. The data points were obtained using equ. (91) to analyze the data published by Kinast et al. [9]. The thermodynamic quantities (S/N) and E_0/E_F were taken from [22]. The solid red and blue lines show the expected low and high temperature limits. Both theory curves include relaxation time effects. The blue dashed curve is a phenomenological two-component model explained in the text.
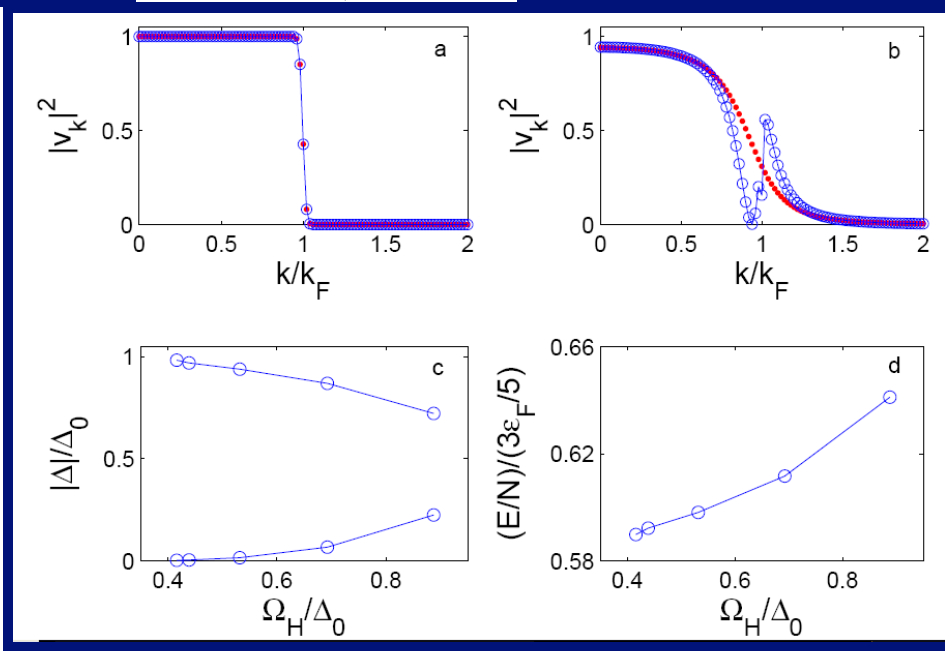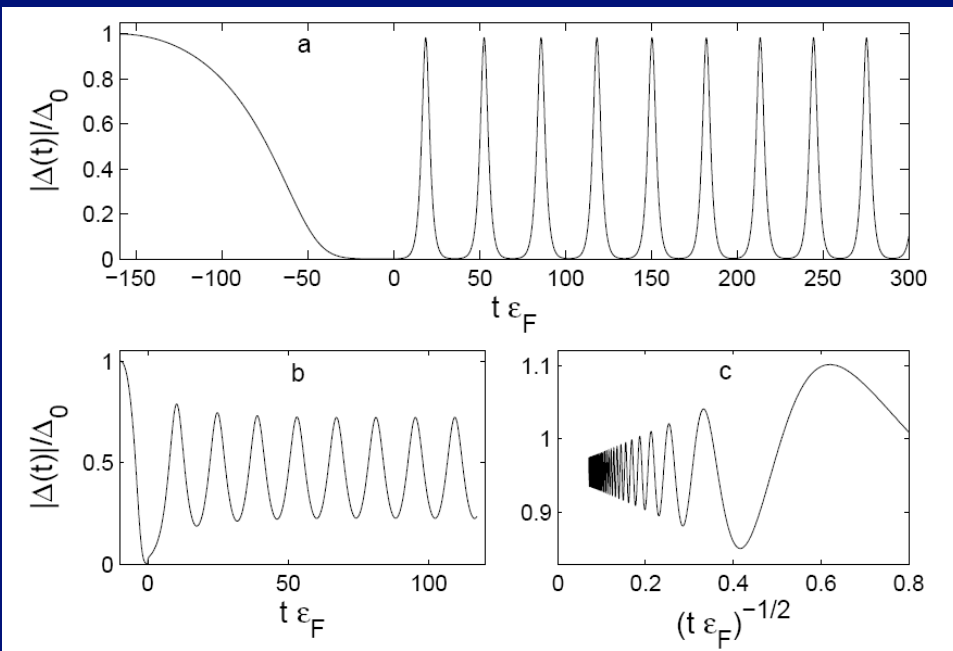
Schaefer and Chafin, chapter in *BCS-BEC crossover and Unitary Fermi Gas,* Lect. Notes in Phys. ed. Zwerger, Springer (2012)

Wlazlowski, Magierski, and Drut, Phys. Rev. Lett. 109, 020406 (2012)
Enss, Haussmann, and Zwerger, Ann. Phys. 326, 770 (2011)
Kovtun, Son, and Starinets (KSS), Phys. Rev. Lett. 94, 111601 (2005)

The Higgs mode
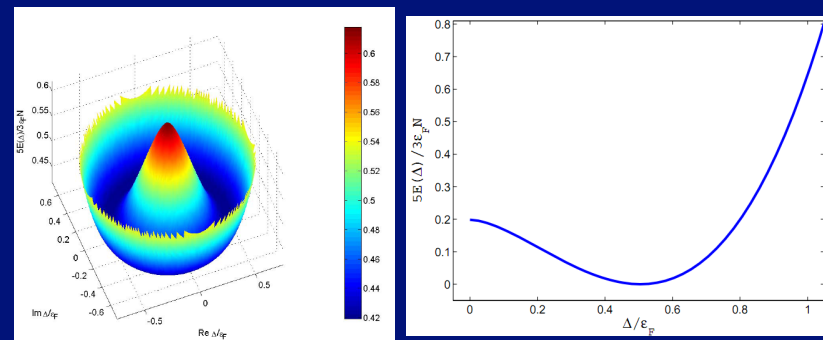
- **All these modes have a very low frequency below the pairing gap, a very large amplitude and very large excitation energy**

- **None of these modes can be described either within two-fluid hydrodynamics or Landau-Ginzburg like approaches**

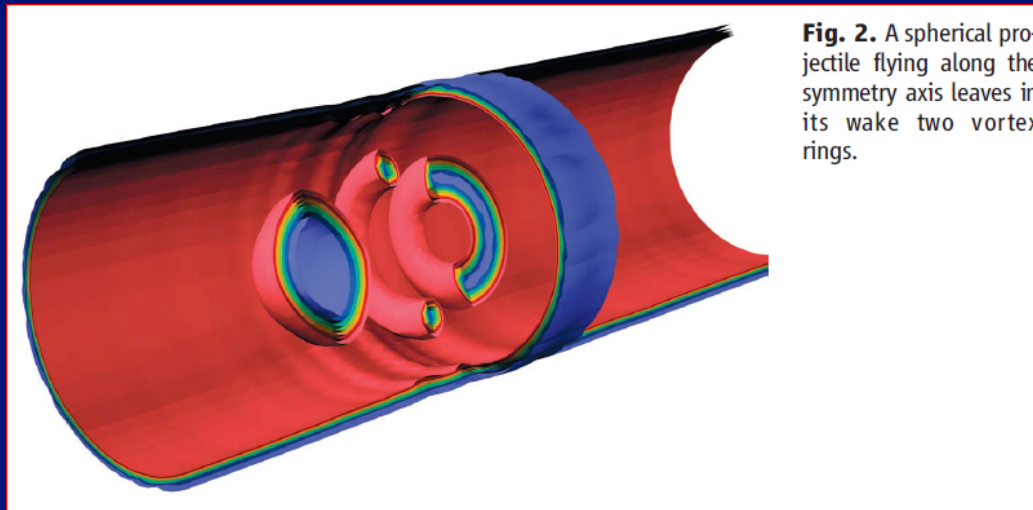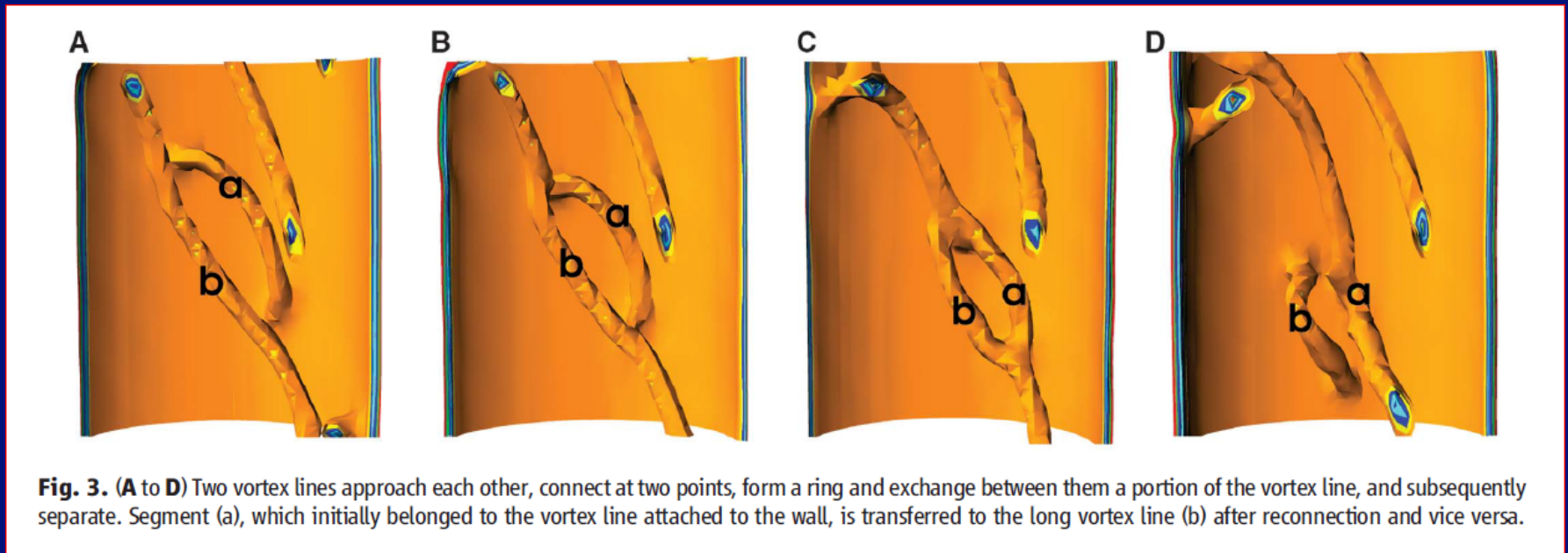**Fig. 2.** A spherical projectile flying along the symmetry axis leaves in its wake two vortex rings.

Onset of quantum turbulence in a fermionic superfluid, conjectured by Feynman (1956)

Fig. 3. (**A** to **D**) Two vortex lines approach each other, connect at two points, form a ring and exchange between them a portion of the vortex line, and subsequently separate. Segment (a), which initially belonged to the vortex line attached to the wall, is transferred to the long vortex line (b) after reconnection and vice versa.

Real-time dynamics of quantized vortices in a unitary Fermi gas
Bulgac, Luo, Magierski, Roche, and Yu, Science, 332, 1288(2011)
and about 4 hours of video at http://www.phys.washington.edu/groups/qmbnt/UFG
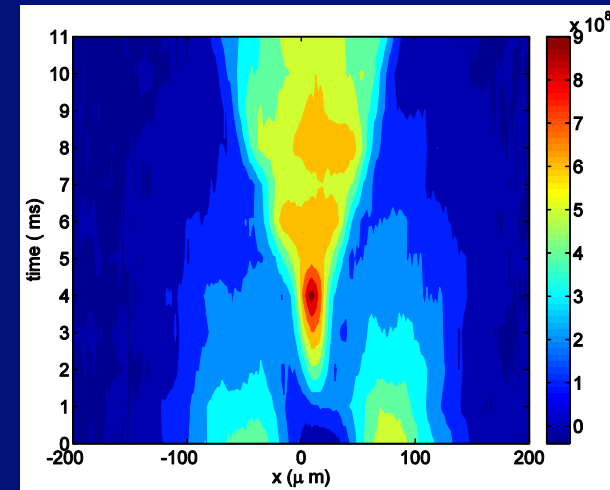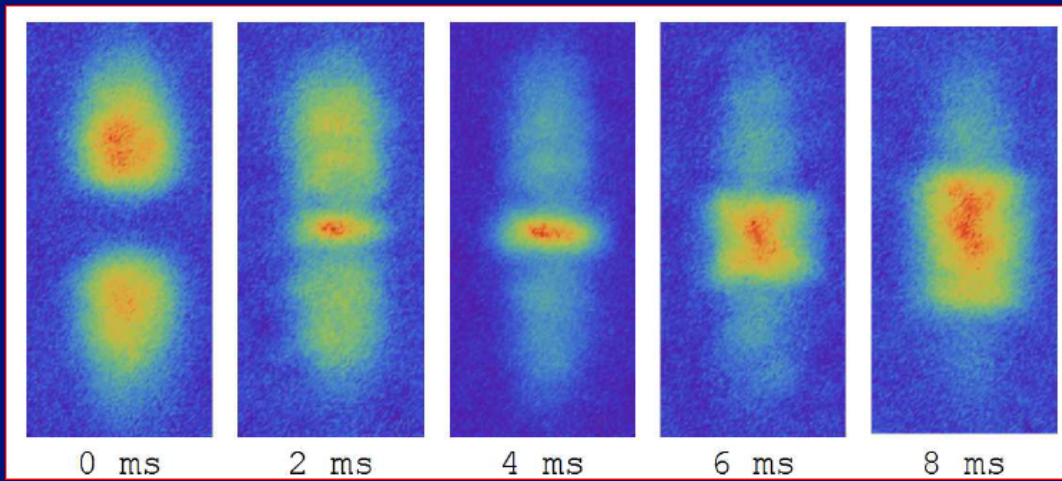
Observation of shock waves in a strongly interacting Fermi gas
Joseph, Thomas, Kulkarni, and Abanov, Phys. Rev. Lett. 106, 150401 (2011)
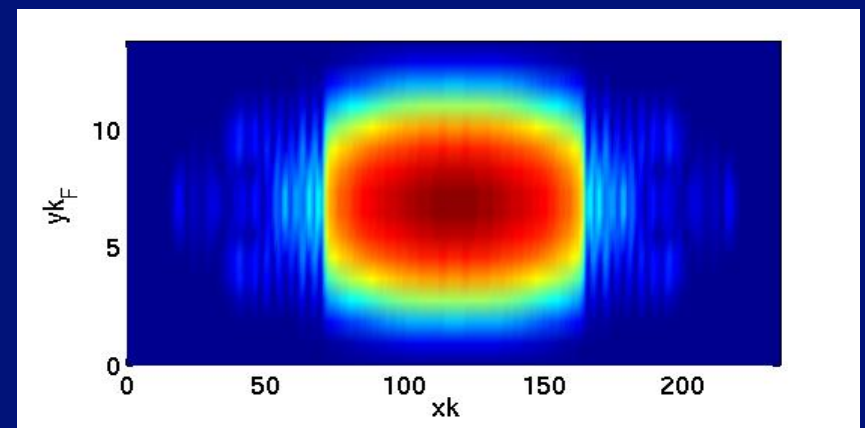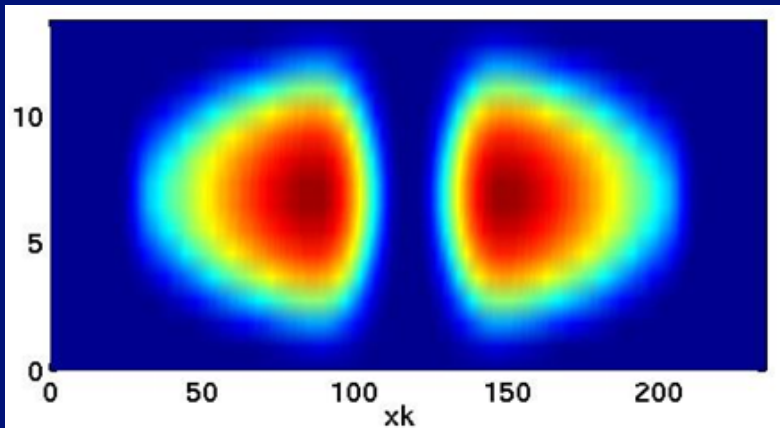
**Number density of two colliding cold Fermi gases in TDSLDA
Bulgac, Luo, and Roche, Phys. Rev. Lett. 108, 150401 (2012)**

Dark solitons/domain walls and shock waves in the collision of two UFG clouds (about 750 fermions, TDSLDA (superfluid extension of TDDFT) calculation)
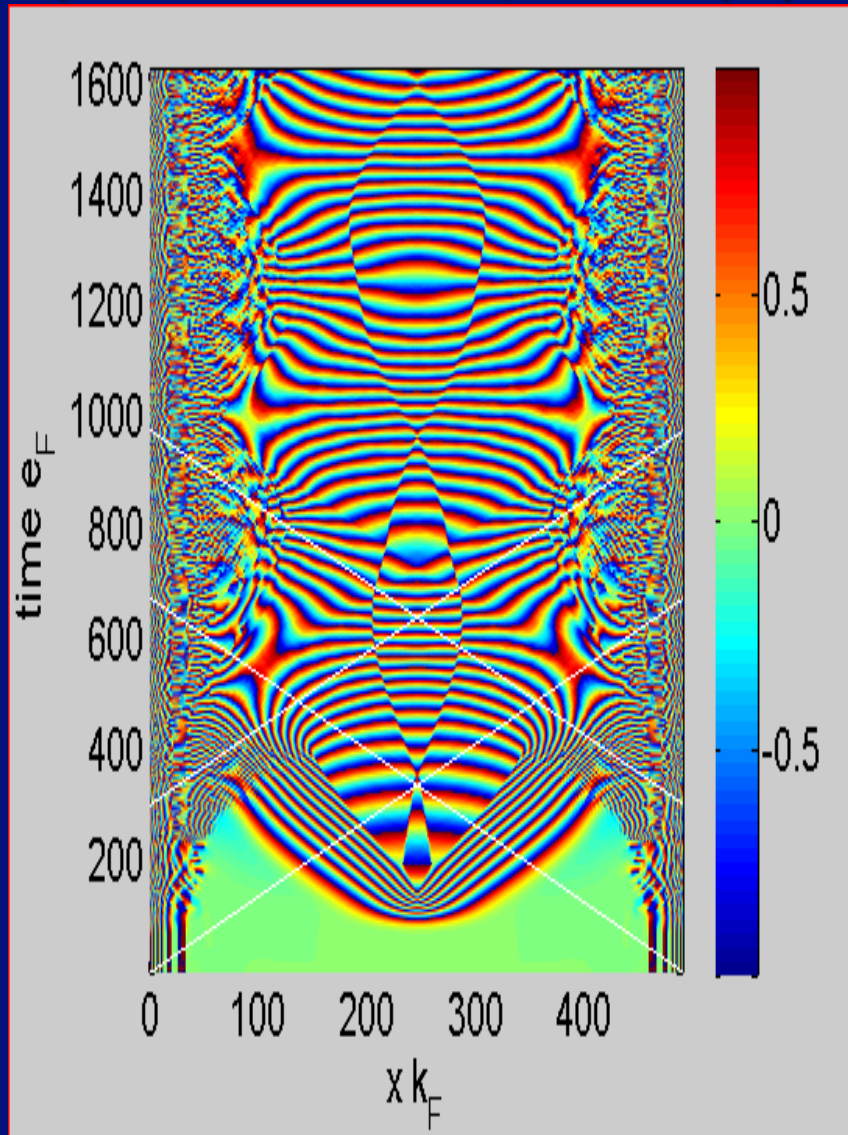
Phase of the pairing gap normalized to ε_F
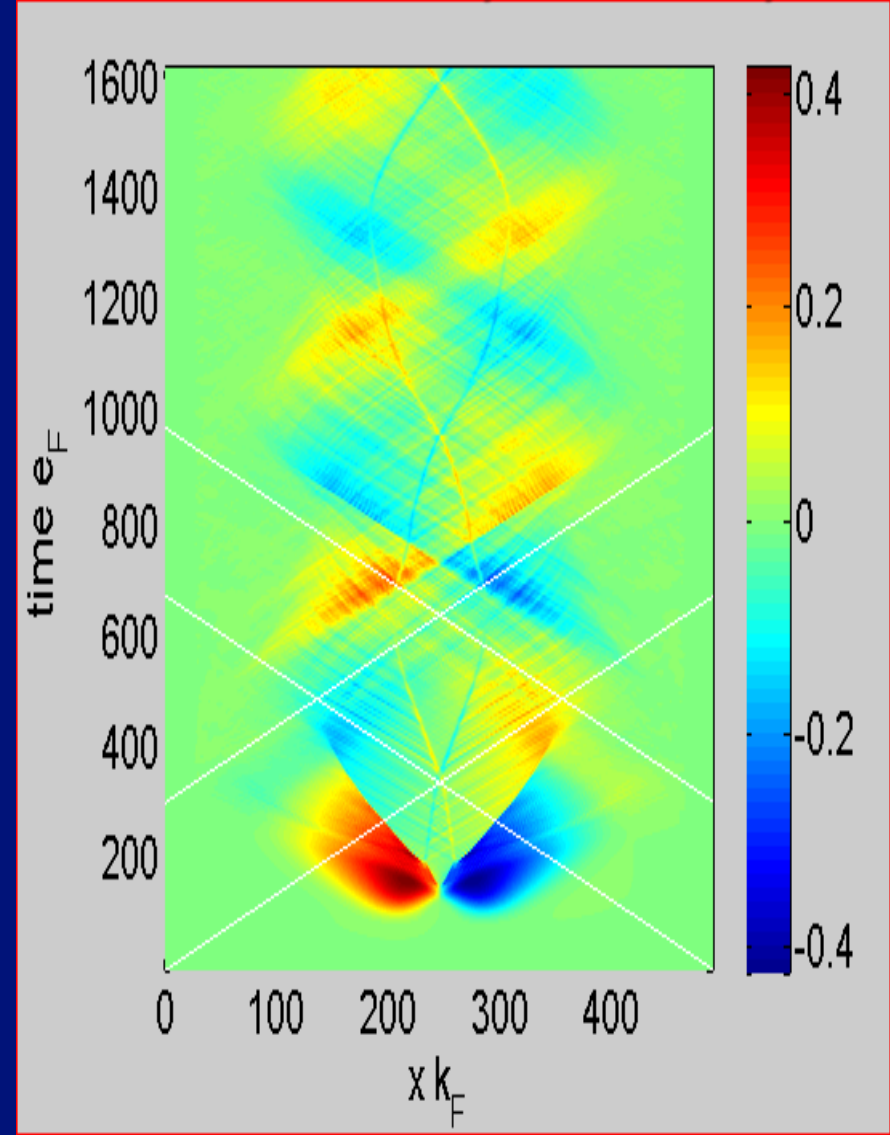
Local velocity normalized to Fermi velocity

Bulgac, Luo, and Roche, Phys. Rev. Lett. 108, 150401 (2012)

What is happening in spin imbalanced systems?

Induced P-wave superfluidity *(even though fermions interact in s-wave only)*
Two new superfluid phases where before they were not expected
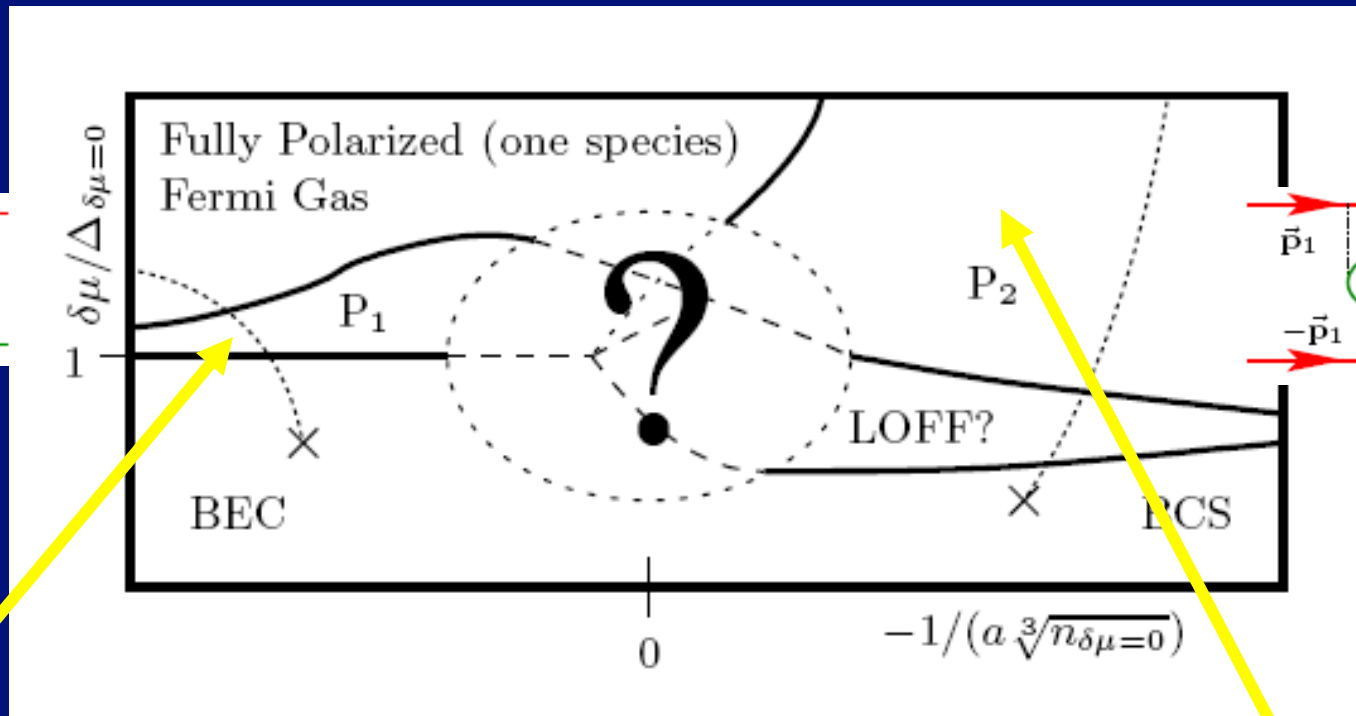
One Bose superfluid coexisting with one P-wave Fermi superfluid

Two coexisting P-wave Fermi superfluids

Asymmetric Fermi gas at unitarity
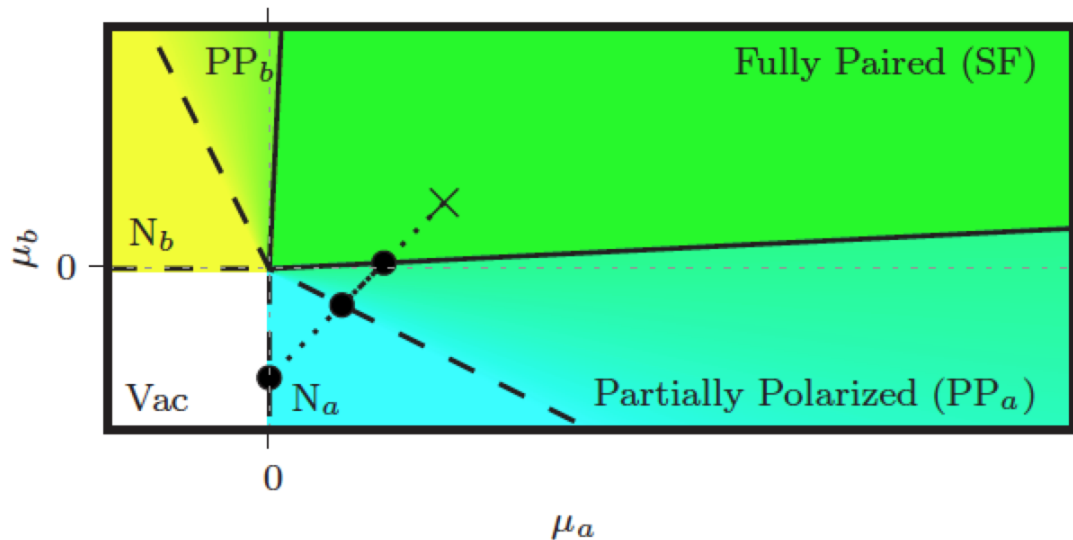
FIG. 1. (Color online) Grand-canonical phase diagram of a two-component Fermi gas at unitarity and $T=0$. Various phases are separated by phase transitions along the straight lines extending from the origin with constant slopes y_x. The dotted line follows the sequence of phases in a sample trap.

$$\Omega = -VP(\mu_\uparrow, \mu_\downarrow) = \frac{1}{6\pi^2}\left[\frac{2m}{\hbar^2}\right]^{3/2}\left[\mu_\uparrow h\left(\frac{\mu_\downarrow}{\mu_\uparrow}\right)\right]^{5/2}$$

Dimensional arguments and Legendre transform for unitary Fermi gas

$$P(\mu_\uparrow, \mu_\downarrow) = \mu_\uparrow n_\uparrow + \mu_\downarrow n_\downarrow - \varepsilon(n_\uparrow, n_\downarrow) = \frac{2}{3}\varepsilon(n_\uparrow, n_\downarrow)$$

$$P(\mu_\uparrow, \mu_\downarrow) = \frac{2}{5}\beta\left[\mu_\uparrow h\left(\frac{\mu_\downarrow}{\mu_\uparrow}\right)\right]^{5/2}, \quad \beta = \frac{1}{6\pi^2}\left[\frac{2m}{\hbar^2}\right]^{3/2}$$

$$\varepsilon(n_\uparrow, n_\downarrow) = \frac{3}{5}\alpha\left[n_\uparrow g\left(\frac{n_\downarrow}{n_\uparrow}\right)\right]^{5/3}, \quad \alpha = \frac{\left(6\pi^2\right)^{2/3}\hbar^2}{2m}$$

$$h(y) = \begin{cases} 1, & y \le y_0 < 0 \\[2mm] \dfrac{1+y}{(2\xi)^{3/5}}, & y_1 \le y \le 1 \end{cases}$$

$$h''(y) \ge 0$$

$$g(0) = 1, \quad g(1) = (2\xi)^{3/5}$$

$$g''(x) \ge 0$$

$$g'(0) \le Y_0, \quad g'(x) \in g(1)\left[\frac{Y_1}{1+Y_1}, \frac{1}{2}\right]$$

Fully polarized

$$\frac{\mu_\uparrow - \mu_\downarrow}{2} = \Delta$$

FIG. 2. (Color online) Example of a function $h(y)$ and the corresponding function $g(x)$ shown as thick lines. Maxwell's construction for phase coexistence leads to a linear $g(x)$ for $x \in (0.5, 1.0)$, interpolating between the two pure phases shown with lighter lines. This corresponds to the kink and/or first-order phase transition at $y=y_1$ in $h(y)$. Various other sample functions are lightly sketched within the allowed (dotted) triangular region.

From energy of one spin-down particle in a see of spin-ups

$$P_{SF} = \frac{4\beta}{5\xi^{3/2}} \left(\frac{\mu_\uparrow + \mu_\downarrow}{2} \right)^{5/2}$$

Unpolarized SF
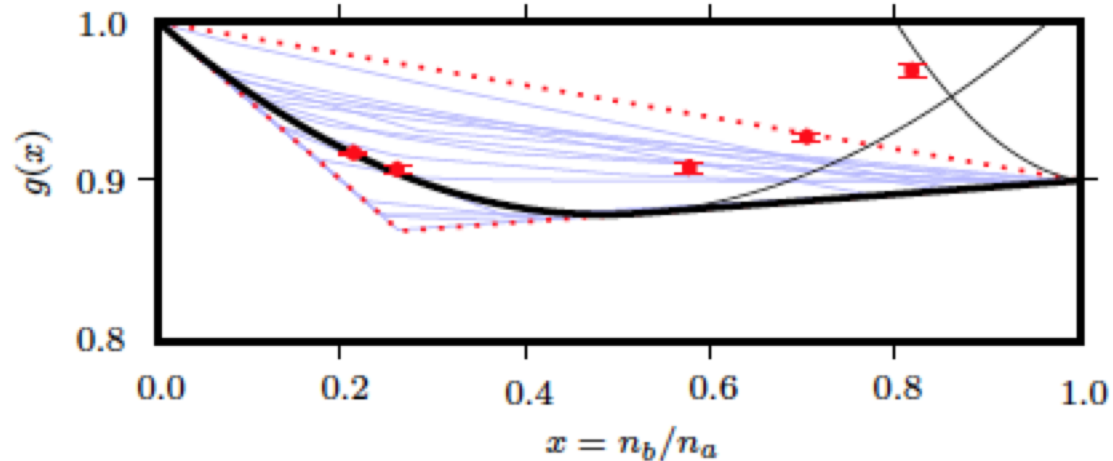
FIG. 7: Monte Carlo variational upper bound on $g(x)$ from [20] plotted on top of the function $g(x)$ from our Figure 2. Note the agreement from small polarizations indicating that our estimate for Y_0 is consistent with their proper variational bound. For larger polarizations, the true curve will lie below the results of Ref. [20] for two reasons: 1) The Maxwell construction for $g(x)$ (see Fig. (2) of [20]) and 2) The authors of Ref. [20] considered only normal Fermi partially polarized states. As shown in [12], at $T = 0$, partially polarized states will be superfluid. This could noticeably lower the energy for substantial polarizations at unitarity.
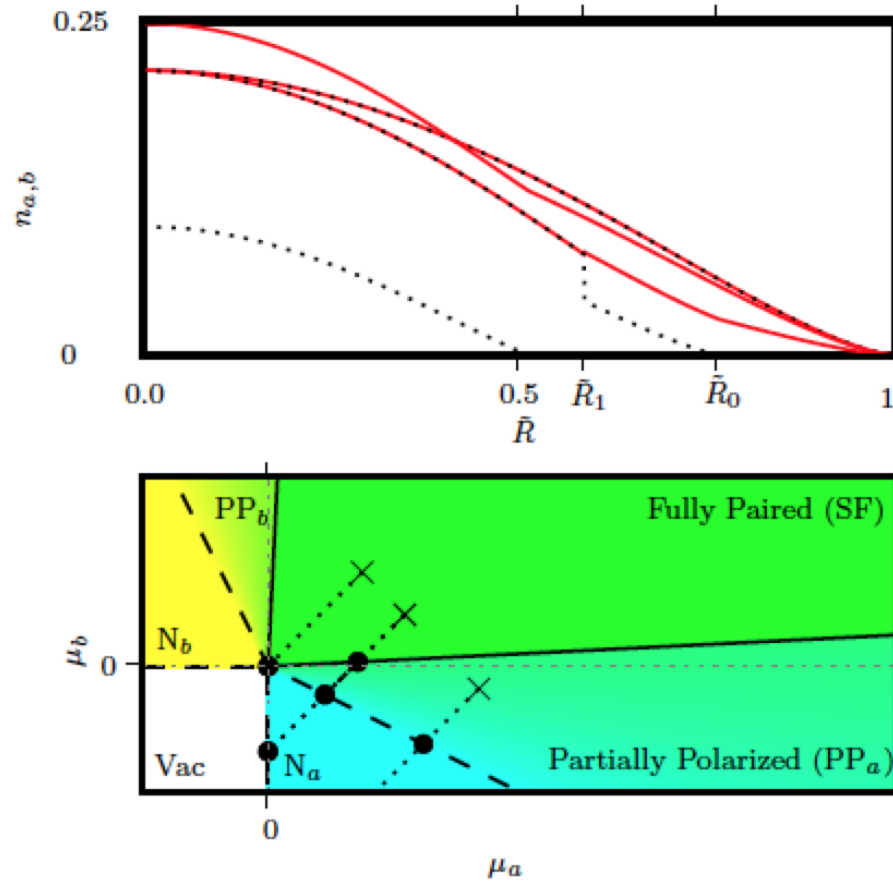
FIG. 5: Density profiles $n_{a,b}$ of the two species in a spherical harmonic trap as a function radius $\tilde{R} = R/R_{vac}$ in units of the cloud radius R_{vac} for thermodynamic function (A22). Density profiles are plotted for a fixed $\lambda_+ = (\lambda_a + \lambda_b)/2$ and a variety of chemical potential differences $\mu_- = \lambda_-$ ranging from $\lambda_- = 0$ (fully paired $n_a = n_b$ throughout the trap) to $\lambda_- = \lambda_+$ (no superfluid core). The red solid lines are the majority species n_a while the black dotted lines are the minority species. The critical radii for the intermediate profile have been denoted $\tilde{R}_{0,1}$.

What is Density Functional Theory (DFT)?

R. M. Dreizler E. K. U. Gross

Density Functional Theory

An Approach to the
Quantum Many-Body Problem
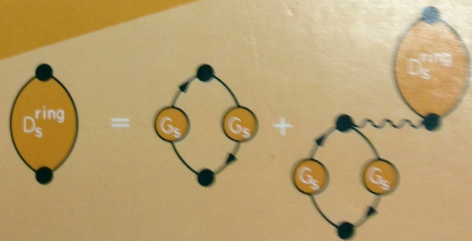
Miguel A. L. Marques
Neepa T. Maitra
Fernando M. S. Nogueira
Eberhard K. U. Gross
Angel Rubio *Editors*

Fundamentals of Time-Dependent Density Functional Theory

However, not everyone is normal!

Kohn-Sham theorem (1965)

$$H = \sum_i^N T(i) + \sum_{i<j}^N U(ij) + \sum_{i<j<k}^N U(ijk) + \ldots + \sum_i^N V_{ext}(i)$$

$$H\Psi_0(1,2,\ldots N) = E_0 \Psi_0(1,2,\ldots N)$$

$$n(\vec{r}) = \left\langle \Psi_0 \left| \sum_i^N \delta(\vec{r} - \vec{r}_i) \right| \Psi_0 \right\rangle$$

Injective map (one-to-one)

$$\Psi_0(1,2,\ldots N) \iff V_{ext}(\vec{r}) \iff n(\vec{r})$$

$$E_0 = \min_{n(\vec{r})} \int d^3r \left\{ \frac{\hbar^2}{2m^*(\vec{r})} \tau(\vec{r}) + \varepsilon\left[n(\vec{r})\right] + V_{ext}(\vec{r})n(\vec{r}) \right\}$$

$$n(\vec{r}) = \sum_i^N \left|\varphi_i(\vec{r})\right|^2, \qquad \tau(\vec{r}) = \sum_i^N \left|\vec{\nabla}\varphi_i(\vec{r})\right|^2$$

Universal functional of particle density alone
Independent of external potential

Normal Fermi systems only!

The SLDA (DFT) energy density functional at unitarity for equal numbers of spin-up and spin-down fermions

Dimensional arguments, renormalizability, and Galilean invariance determine the functional (energy density)

$$\varepsilon(\vec{r}) = \frac{\hbar^2}{m}\left\{\left[\alpha\,\frac{\tau_c(\vec{r})}{2} - \Delta(\vec{r})\nu_c(\vec{r})\right] + \beta\,\frac{3(3\pi^2)^{2/3}n^{5/3}(\vec{r})}{5}\right\}$$

$$+ \frac{\hbar^2}{m}(\alpha - 1)\frac{\vec{j}^2(\vec{r})}{2n(\vec{r})}$$

$$n(\vec{r}) = 2\sum_{0<E_k<E_c}\left|\mathrm{v}_k(\vec{r})\right|^2, \quad \tau_c(\vec{r}) = 2\sum_{0<E_k<E_c}\left|\vec{\nabla}\mathrm{v}_k(\vec{r})\right|^2,$$

$$\nu_c(\vec{r}) = \sum_{0<E<E_c}\mathrm{u}_k(\vec{r})\mathrm{v}_k^*(\vec{r})$$

Three dimensionless constants α, β, and γ determining the functional are extracted from QMC for homogeneous systems by fixing the total energy, the pairing gap and the effective mass

Formalism for Time-Dependent Phenomena

"The time-dependent density functional theory is viewed in general as a reformulation of the exact quantum mechanical time evolution of a many-body system when only one-body properties are considered."

A.K. Rajagopal and J. Callaway, Phys. Rev. B **7**, 1912 (1973)
V. Peuckert, J. Phys. C **11**, 4945 (1978)
E. Runge and E.K.U. Gross, Phys. Rev. Lett. **52**, 997 (1984)

http://www.tddft.org

$$E(t) = \int d^3r \left[\varepsilon(n(\vec{r},t), \tau(\vec{r},t), \nu(\vec{r},t), \vec{j}(\vec{r},t)) + V_{ext}(\vec{r},t)n(\vec{r},t) + \ldots \right]$$

$$\begin{cases} [h(\vec{r},t) + V_{ext}(\vec{r},t) - \mu]u_i(\vec{r},t) + [\Delta(\vec{r},t) + \Delta_{ext}(\vec{r},t)]v_i(\vec{r},t) = i\hbar \frac{\partial u_i(\vec{r},t)}{\partial t} \\ \\ [\Delta^*(\vec{r},t) + \Delta_{ext}^*(\vec{r},t)]u_i(\vec{r},t) - [h(\vec{r},t) + V_{ext}(\vec{r},t) - \mu]v_i(\vec{r},t) = i\hbar \frac{\partial v_i(\vec{r},t)}{\partial t} \end{cases}$$

For time-dependent phenomena one has to add currents.
Galilean invariance determines the dependence on currents.

Quasiparticle spectrum in homogeneous matter
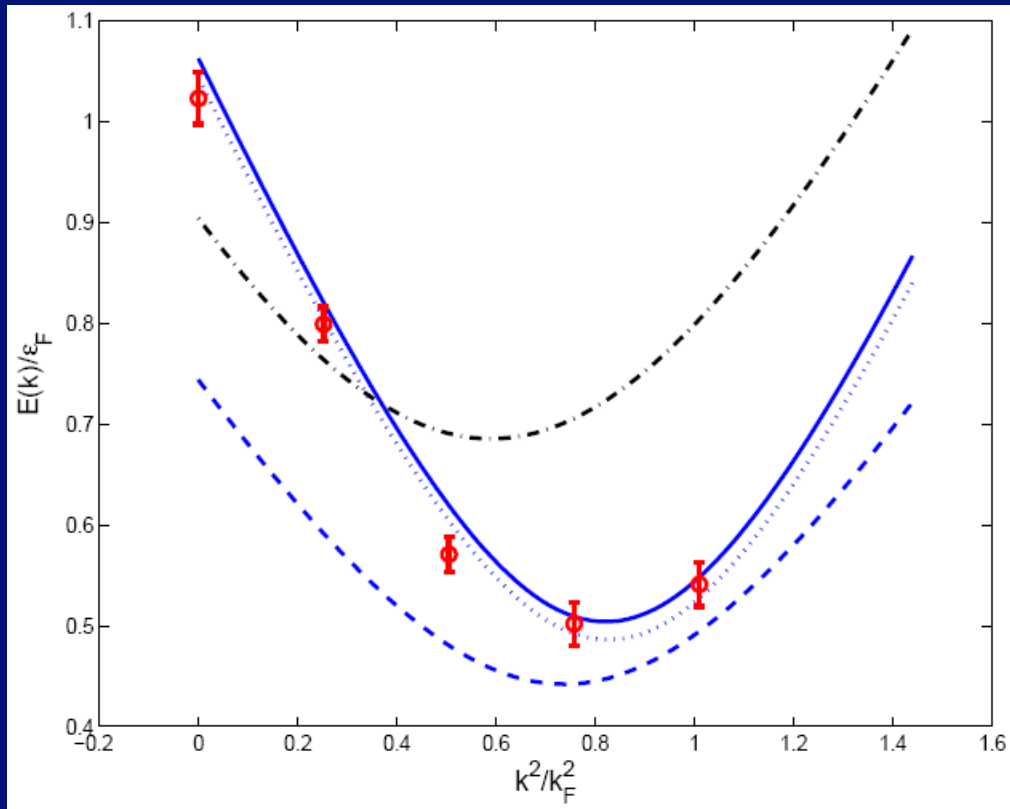
solid/dotted blue line   - SLDA based on homogeneous GFMC due to Carlson *et al*
red circles   - GFMC due to Carlson and Reddy
dashed blue line   - SLDA, homogeneous MC due to Juillet

black dashed-dotted line – meanfield at unitarity

Asymmetric Superfluid Local Density Approximation

$$\Omega = -\int d^3r \left[\varepsilon(\vec{r}) - \mu_\uparrow n_\uparrow(\vec{r}) - \mu_\downarrow n_\downarrow(\vec{r}) - V_{ext}(\vec{r})n_\uparrow(\vec{r}) - V_{ext}(\vec{r})n_\downarrow(\vec{r}) \right]$$

$$\varepsilon(\vec{r}) = \frac{\hbar^2}{2m}\left[\alpha_\uparrow(\vec{r})\tau_\uparrow(\vec{r}) + \alpha_\downarrow(\vec{r})\tau_\downarrow(\vec{r}) \right] + \frac{3\left(3\pi^2\right)^{2/3}\hbar^2}{10m}\left[n_\uparrow(\vec{r}) + n_\downarrow(\vec{r}) \right]^{5/3}\beta(\vec{r}) + g_{eff}(\vec{r})\left| \upsilon(\vec{r}) \right|^2$$

$$n_\uparrow(\vec{r}) = \sum_{E_n<0}\left| \mathrm{u}_n(\vec{r}) \right|^2, \quad n_\downarrow(\vec{r}) = \sum_{E_n<0}\left| \mathrm{v}_n(\vec{r}) \right|^2, \quad \upsilon(\vec{r}) = \frac{1}{2}\sum_{E_n}\mathrm{sgn}(E_n)\mathrm{u}_n(\vec{r})\mathrm{v}_n^*(\vec{r}),$$

$$\tau_\uparrow(\vec{r}) = \sum_{E_n<0}\left| \vec{\nabla}\mathrm{u}_n(\vec{r}) \right|^2, \quad \tau_\downarrow(\vec{r}) = \sum_{E_n<0}\left| \vec{\nabla}\mathrm{v}_n(\vec{r}) \right|^2,$$

$$\alpha_\uparrow(\vec{r}) = \alpha\left[\frac{n_\downarrow(\vec{r})}{n_\uparrow(\vec{r})}\right], \quad \alpha_\downarrow(\vec{r}) = \alpha\left[\frac{n_\uparrow(\vec{r})}{n_\downarrow(\vec{r})}\right], \quad \beta(\vec{r}) = \beta\left[\frac{n_\downarrow(\vec{r})}{n_\uparrow(\vec{r})}\right] = \beta\left[\frac{n_\uparrow(\vec{r})}{n_\downarrow(\vec{r})}\right],$$

$$\begin{pmatrix} T_\uparrow(\vec{r}) + U_\uparrow(\vec{r}) - \mu_\uparrow & \Delta(\vec{r}) \\ \Delta^*(\vec{r}) & -T_\downarrow(\vec{r}) - U_\downarrow(\vec{r}) + \mu_\downarrow \end{pmatrix}\begin{pmatrix} \mathrm{u}_n(\vec{r}) \\ \mathrm{v}_n(\vec{r}) \end{pmatrix} = E_n\begin{pmatrix} \mathrm{u}_n(\vec{r}) \\ \mathrm{v}_n(\vec{r}) \end{pmatrix}$$

Normal State				Superfluid State			
(N_a, N_b)	E_{FNDMC}	E_{ASLDA}	(error)	(N_a, N_b)	E_{FNDMC}	E_{ASLDA}	(error)
(3,1)	6.6 ± 0.01	6.687	1.3%	(1,1)	2.002 ± 0	2.302	15%
(4,1)	8.93 ± 0.01	8.962	0.36%	(2,2)	5.051 ± 0.009	5.405	7%
(5,1)	12.1 ± 0.1	12.22	0.97%	(3,3)	8.639 ± 0.03	8.939	3.5%
(5,2)	13.3 ± 0.1	13.54	1.8%	(4,4)	12.573 ± 0.03	12.63	0.48%
(6,1)	15.8 ± 0.1	15.65	0.93%	(5,5)	16.806 ± 0.04	16.19	3.7%
(7,2)	19.9 ± 0.1	20.11	1.1%	(6,6)	21.278 ± 0.05	21.13	0.69%
(7,3)	20.8 ± 0.1	21.23	2.1%	(7,7)	25.923 ± 0.05	25.31	2.4%
(7,4)	21.9 ± 0.1	22.42	2.4%	(8,8)	30.876 ± 0.06	30.49	1.2%
(8,1)	22.5 ± 0.1	22.53	0.14%	(9,9)	35.971 ± 0.07	34.87	3.1%
(9,1)	25.9 ± 0.1	25.97	0.27%	(10,10)	41.302 ± 0.08	40.54	1.8%
(9,2)	26.6 ± 0.1	26.73	0.5%	(11,11)	46.889 ± 0.09	45	4%
(9,3)	27.2 ± 0.1	27.55	1.3%	(12,12)	52.624 ± 0.2	51.23	2.7%
(9,5)	30 ± 0.1	30.77	2.6%	(13,13)	58.545 ± 0.18	56.25	3.9%
(10,1)	29.4 ± 0.1	29.41	0.034%	(14,14)	64.388 ± 0.31	62.52	2.9%
(10,2)	29.9 ± 0.1	30.05	0.52%	(15,15)	70.927 ± 0.3	68.72	3.1%
(10,6)	35 ± 0.1	35.93	2.7%	(1,0)	1.5 ± 0.0	1.5	0%
(20,1)	73.78 ± 0.01	73.83	0.061%	(2,1)	4.281 ± 0.004	4.417	3.2%
(20,4)	73.79 ± 0.01	74.01	0.3%	(3,2)	7.61 ± 0.01	7.602	0.1%
(20,10)	81.7 ± 0.1	82.57	1.1%	(4,3)	11.362 ± 0.02	11.31	0.49%
(20,20)	109.7 ± 0.1	113.8	3.7%	(7,6)	24.787 ± 0.09	24.04	3%
(35,4)	154 ± 0.1	154.1	0.078%	(11,10)	45.474 ± 0.15	43.98	3.3%
(35,10)	158.2 ± 0.1	158.6	0.27%	(15,14)	69.126 ± 0.31	62.55	9.5%
(35,20)	178.6 ± 0.1	180.4	1%				

Bulgac, Forbes, and Magierski, Lecture Notes in Physics (2012)

EOS for spin polarized systems
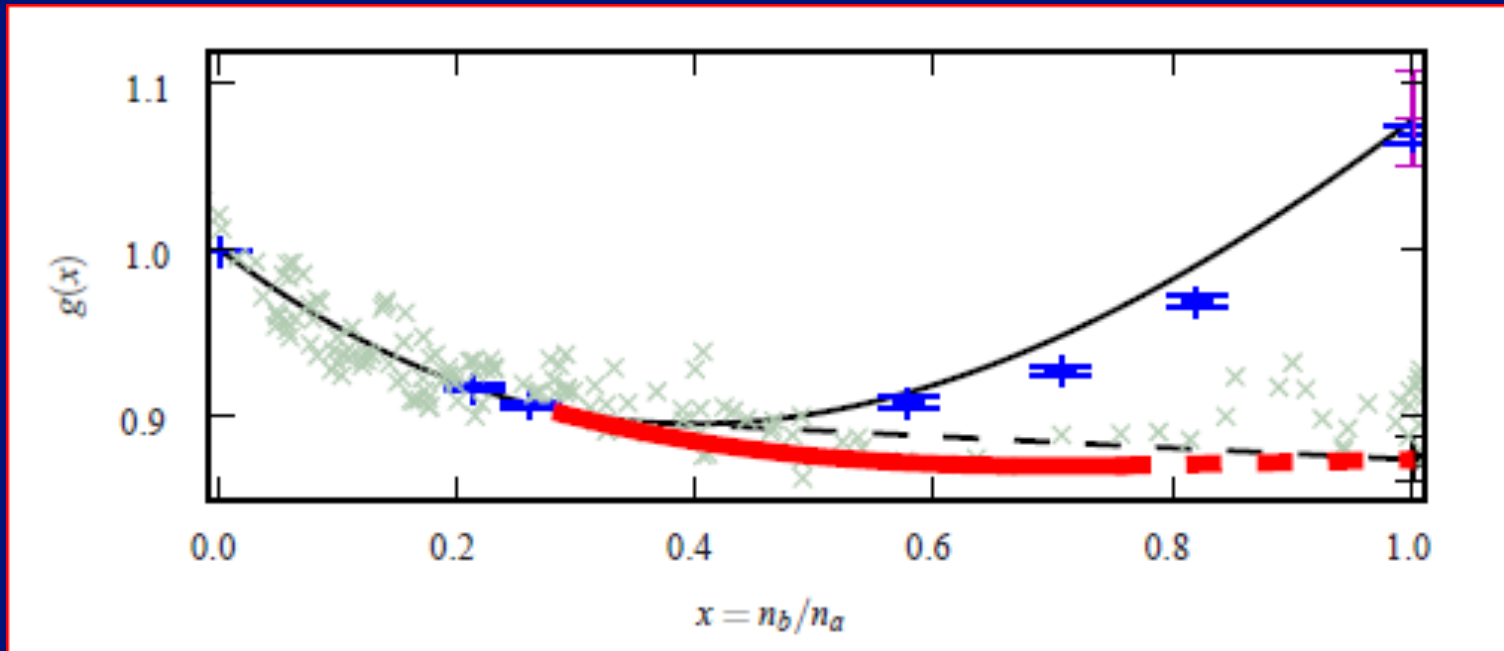
Red line: Larkin-Ovchinnikov phase (unitary Fermi supersolid)

Black line: normal part of the energy density
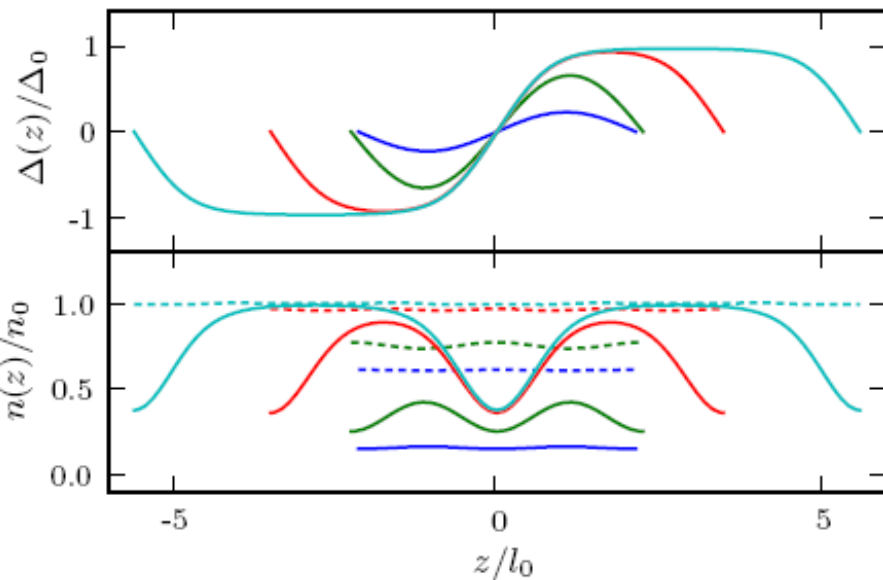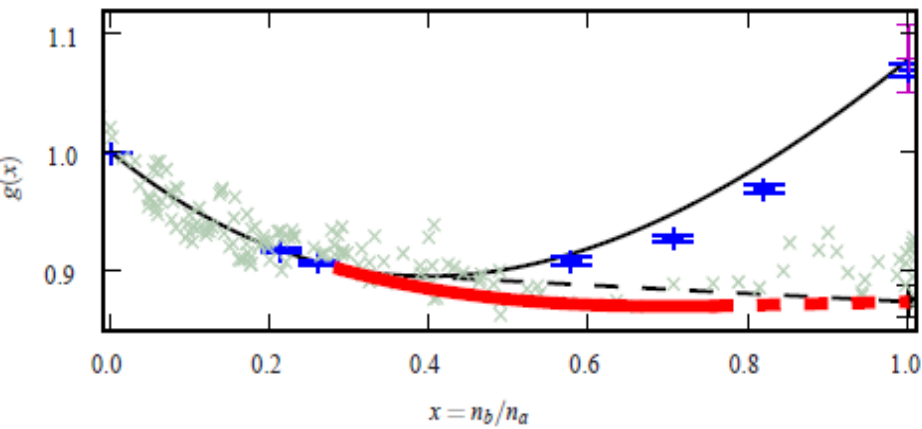Blue points: DMC calculations for normal state, Lobo et al, PRL **97**, 200403 (2006)
Gray crosses: experimental EOS due to Shin, Phys. Rev. A 77, 041603(R) (2008)

$$E(n_a, n_b) = \frac{3}{5} \frac{(6\pi^2)^{2/3} \hbar^2}{2m} \left[n_a g\left(\frac{n_b}{n_a}\right) \right]^{5/3}$$
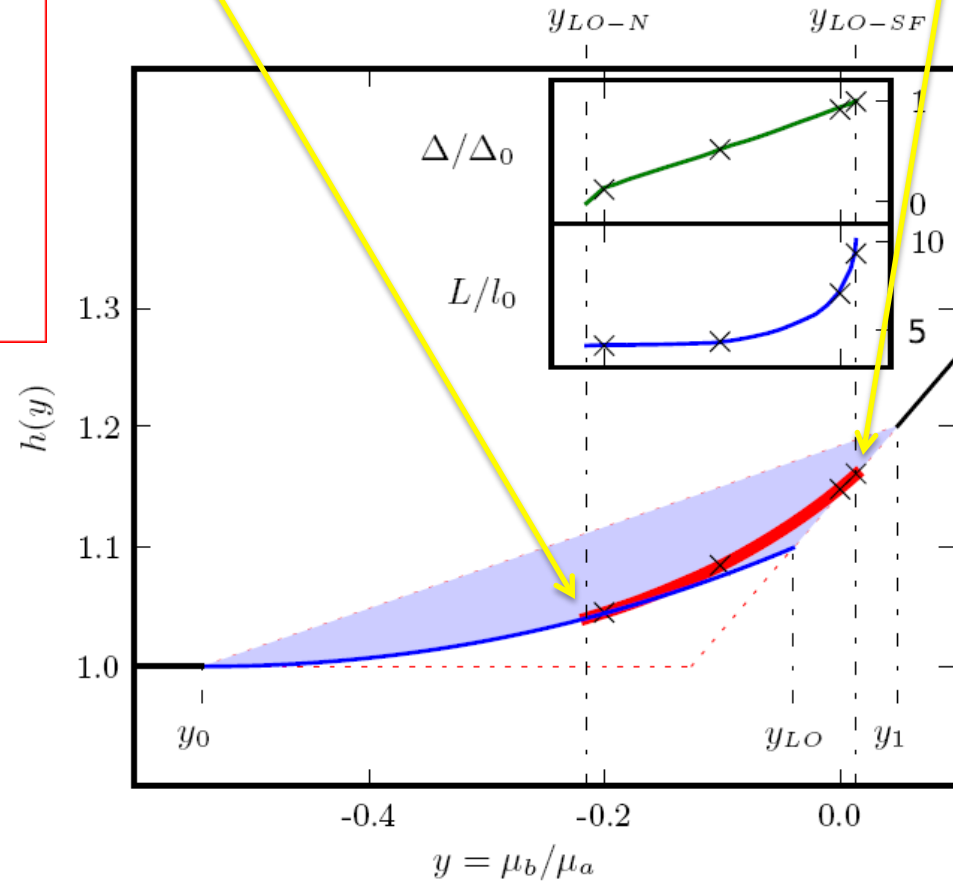
Bulgac and Forbes,
Phys. Rev. Lett. **101**, 215301 (2008)

A Unitary Fermi Supersolid: the Larkin-Ovchinnikov phase

Second order phase transition

First order phase transition
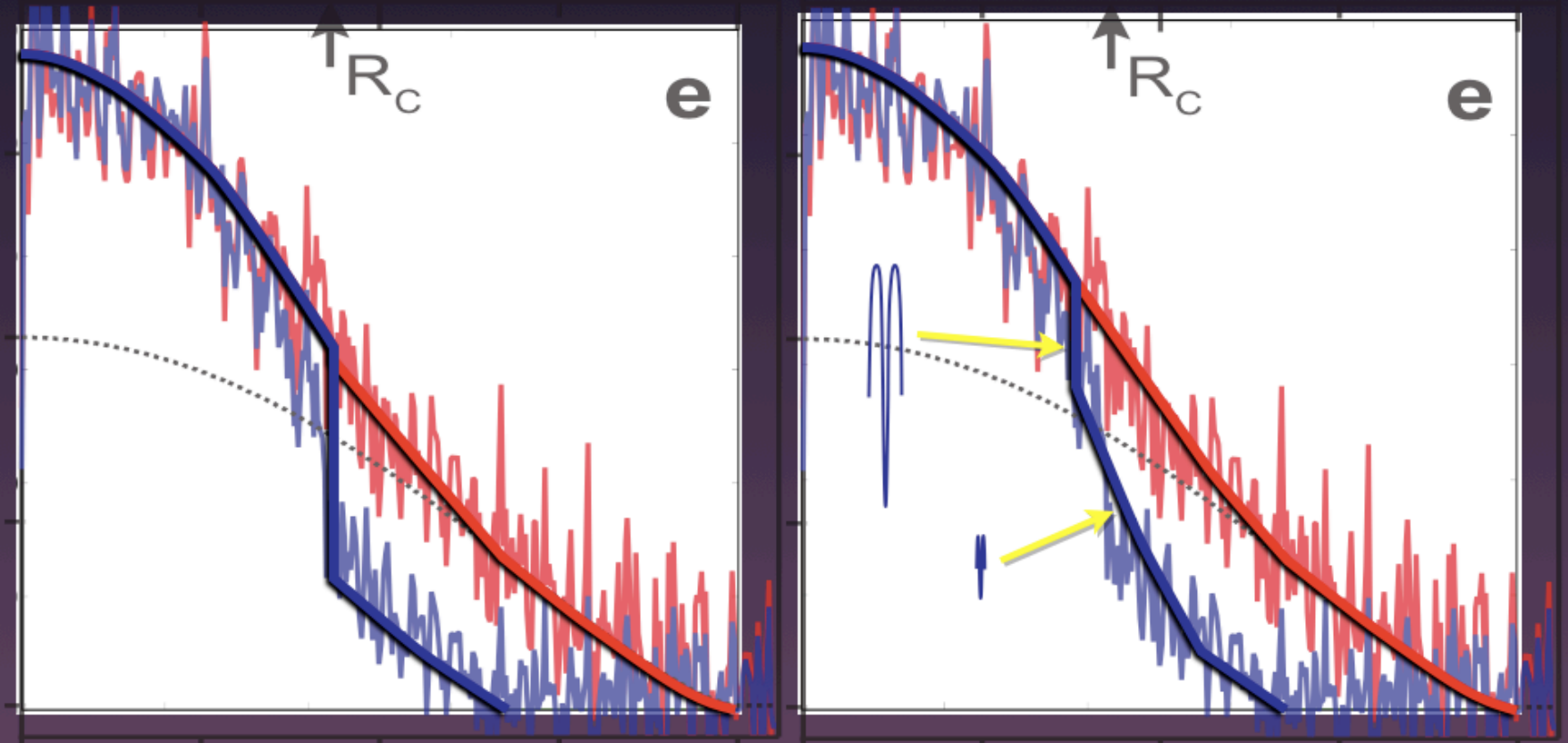

**Bulgac and Forbes
Phys. Rev. Lett. 101, 215301 (2008)**

NB This is a gas system at the same time!

$$P[\mu_a, \mu_b] = \frac{2}{30\pi^2}\left(\frac{2m}{\hbar^2}\right)^{3/2}\left[\mu_a h\left(\frac{\mu_b}{\mu_a}\right)\right]^{5/2}$$

Observations: Inconclusive

- Need detailed structure or novel signature

MIT Experimental data from Shin et. al (2008)